
FOCUS: Fairness via Agent-Awareness for Federated Learning on Heterogeneous Data

Wenda Chu^{*1} Chulin Xie^{*2} Boxin Wang² Linyi Li² Lang Yin² Arash Nourian³ Han Zhao² Bo Li²

Abstract

Federated learning (FL) allows agents to jointly train a global model without sharing their local data. However, due to the heterogeneous nature of local data, existing definitions of fairness in the context of FL are prone to noisy agents in the network. For instance, existing work usually considers accuracy parity as fairness for different agents in FL, which is not robust under the heterogeneous setting, since it will enforce agents with high-quality data to achieve similar accuracy to those who contribute low-quality data, which may discourage the benign agents from participating in FL. In this work, we propose a formal FL fairness definition, *fairness via agent-awareness* (FAA), which takes the heterogeneity of different agents into account. Under FAA, the performance of agents with high-quality data will not be sacrificed just due to the existence of large numbers of agents with low-quality data. In addition, we propose a fair FL training algorithm based on agent clustering (FOCUS) to achieve fairness in FL, as measured by FAA. Theoretically, we prove the convergence and optimality of FOCUS under mild conditions for both linear and general convex loss functions with bounded smoothness. We also prove that FOCUS always achieves higher fairness in terms of FAA compared with standard FedAvg under both linear and general convex loss functions. Empirically, we show that on four FL datasets, including synthetic data, images, and texts, FOCUS achieves significantly higher fairness in terms of FAA while maintaining competitive prediction accuracy compared with FedAvg and state-of-the-art fair FL algorithms.

1. Introduction

Federated learning (FL) is emerging as a promising approach to enable scalable intelligence over distributed settings such as mobile networks (Lim et al., 2020; Hard et al., 2018). Given the wide adoption of FL in medical analysis (Sheller et al., 2020; Adnan et al., 2022), recommendation systems (Minto et al., 2021; Anelli et al., 2021), and personal Internet of Things (IoT) devices (Alawadi et al., 2021), it has become a central question on how to ensure the fairness of the trained global model in FL networks before its large-scale deployment by local agents, especially when the data quality/contributions of different agents are different in the heterogeneous setting.

In standard (centralized) ML, fairness is usually defined as a notion of parity of the underlying distributions from different groups given by a protected attribute (e.g., gender, race). Typical definitions include demographic parity (Zemel et al., 2013; Dwork et al., 2012), equalized odds (Hardt et al., 2016), and accuracy parity (Buolamwini & Gebru, 2018; Zhao & Gordon, 2022). However, it is yet unclear what is the desired notion of fairness in FL. Previous works that explore fairness in FL mainly focus on the demographic disparity of the final trained model regarding the protected attributes without considering different contributions of agents (Chu et al., 2021; Hu et al., 2022) or the accuracy disparity across agents (Li et al., 2020b; Donahue & Kleinberg, 2022a; Mohri et al., 2019). Some works have taken into consideration the local data properties (Zhang et al., 2020; Kang et al., 2019) and data size (Donahue & Kleinberg, 2022b). However, the fairness analysis in FL under heterogeneous agent contributions is still lacking. Thus, in this paper, we aim to ask: *What is a desirable notion of fairness in FL?* On one hand, it should be able to take the heterogeneity of different local agents into account so that it is robust to the potential noisy nodes in the network. On the other hand, it should also encourage the participation of benign agents that contribute high-quality data to the FL network. Furthermore, *can we design efficient training algorithms to guarantee it?*

In light of the above questions, in this work, we aim to define and enhance fairness by explicitly considering the heterogeneity of local agents. In particular, for FL trained

^{*}Equal contribution ¹ California Institute of Technology
²University of Illinois Urbana-Champaign ³Amazon.

with standard FedAvg protocol (McMahan et al., 2017), if we denote the data of agent e as D_e with size n_e and the total number of data as n , the final trained global model aims to minimize the loss with respect to the global distribution $\mathcal{P} = \sum_{e=1}^E \frac{n_e}{n} D_e$, where E is the total number of agents. In practice, some local agents may have low-quality data (e.g., free riders), so intuitively it is “unfair” to train the final model regarding such global distribution over all agents, which will sacrifice the performance of agents with high-quality data. For example, considering the FL applications for medical analysis, some hospitals have high-resolution medical data with fine-grained labels, which are expensive to collect; some hospitals may only be able to provide low-resolution medical data and noisy labels. In such a setting, the utility of agents with high-quality data would be harmed due to the aggregated global distribution. Thus, a proper fairness notion is critical to encourage agents to participate in FL and ensure their utility.

In this paper, we define **fairness via agent-awareness in FL (FAA)** as $\mathcal{FAA}(\{\theta_e\}_{e \in [E]}) = \max_{e_1, e_2 \in E} |\mathcal{E}_{e_1}(\theta_{e_1}) - \mathcal{E}_{e_2}(\theta_{e_2})|$, where \mathcal{E}_e is the *excess risk* of an agent $e \in E$ with model parameter θ_e . Technically, the excess risk of each agent is calculated as $\mathcal{E}_e(\theta_e) = \mathcal{L}_e(\theta_e) - \min_{\theta^*} \mathcal{L}_e(\theta^*)$, which stands for the loss of user e evaluated on the FL model θ_e subtracted by the Bayes optimal error of the local data distribution (Oppor & Haussler, 1991). For each agent, a lower excess risk $\mathcal{E}_e(\theta_e)$ indicates a *higher gain* from the FL model θ_e w.r.t the local distribution because its loss $\mathcal{L}_e(\theta_e)$ is closer to its Bayes optimal error. Notably, reducing FAA enforces the *equity of excess risks* among agents, following the classic philosophy that agents “do not suffer from scarcity, but inequality of gains” (gains in terms of *relative* performance improvement measured by excess risks) from participating in FL. Therefore, lower FAA indicates stronger fairness for FL.

Based on our fairness definition FAA, we then propose a *fair FL algorithm based on agent clustering* (FOCUS) to improve the fairness of FL. Specifically, we first cluster the local agents based on their data distributions and then train a model for each cluster. During inference time, the final prediction will be the weighted aggregation over the prediction result of each model trained with the corresponding clustered local data. Theoretically, we prove that the final converged stationary point of FOCUS is exponentially close to the optimal cluster assignment under mild conditions. In addition, we prove that the fairness of FOCUS in terms of FAA is strictly higher than that of the standard FedAvg under both linear models and general convex losses. Empirically, we evaluate FOCUS on four datasets, including synthetic data, images, and texts, and we show that FOCUS achieves higher fairness measured by FAA than FedAvg and SOTA fair FL algorithms while maintaining similar or even higher prediction accuracy.

Technical contributions. We define and improve FL fairness in heterogeneous settings by considering the different contributions of heterogeneous local agents. We make contributions on both the theoretical and empirical fronts.

- We formally define *fairness via agent-awareness (FAA)* in FL based on agent-level excess risks to measure fairness in FL, and explicitly take the heterogeneity nature of local agents into account.
- We propose a fair FL algorithm via agent clustering (FOCUS) to improve fairness measured by FAA, especially in the heterogeneous setting. We prove the convergence rate and optimality of FOCUS under linear models and general convex losses.
- Theoretically, we prove that FOCUS achieves stronger fairness measured by FAA compared with FedAvg for both linear models and general convex losses.
- Empirically, we compare FOCUS with FedAvg and SOTA fair FL algorithms on four datasets, including synthetic data, images, and texts under heterogeneous settings. We show that FOCUS indeed achieves stronger fairness measured by FAA while maintaining similar or even higher prediction accuracy on all datasets.

2. Related work

Fair Federated Learning There have been several studies exploring fairness in FL. Li et al. first define agent-level fairness by considering *accuracy equity* across agents and achieve fairness by assigning the agents with worse performance with higher aggregation weight during training. However, such a definition of fairness fails to capture the heterogeneous nature of local agents. Mohri et al. pursue accuracy parity by improving the performance of the worst-performing agent. Wang et al. (2021) propose to mitigate conflict gradients from local agents to enhance fairness. Instead of pursuing fairness with one single global model, Li et al. propose to train a personalized model for each agent to achieve accuracy equity for the personalized models. Zhang et al. predefine the agent contribution levels based on an oracle assumption (e.g., data volume, data collection cost, etc.) for fairness optimization, which lacks quantitative measurement metrics in practice. Xu et al. approximate the Shapely Value based on gradient cosine similarity to evaluate agent contribution. However, Zhang et al. point out that Shapely Value may discourage agents with rare data, especially under heterogeneous settings. Here we provide an algorithm to quantitatively measure the contribution of local data based on each agent’s excess risk, which will not be affected even if the agent is the minority.

Clustered Federated Learning Clustered FL algorithms are initially designed for multitasking and personalized federated learning, which assumes that agents can be naturally partitioned into clusters (Ghosh et al., 2020; Xie et al., 2021; Sattler et al., 2021; Marfoq et al., 2021). Existing clustering algorithms usually aim to assign each agent to a cluster that

provides the lowest loss (Ghosh et al., 2020), optimize the clustering center to be close to the local model (Xie et al., 2021), or cluster agents with similar gradient updates (with respect to, e.g., cosine similarity (Sattler et al., 2021)) to the same cluster. In addition to these hard clustering approaches (i.e., each agent only belongs to one cluster), soft clustering has also been studied (Marfoq et al., 2021; Li et al., 2022; Ruan & Joe-Wong, 2022; Stallmann & Wilbik, 2022), which enables the agents to benefit from multiple clusters. However, none of these works considers the fairness of clustered FL and the potential implications, and our work makes the first attempt to bridge them.

3. Fair Federated Learning on Heterogeneous Data

We first define our fairness via agent-awareness in FL with heterogeneous data and then introduce our fair FL based on the agent clustering (FOCUS) algorithm to achieve FAA.

3.1. Fairness via Agent-Awareness in FL (FAA)

Given a set of E agents participating in the FL network, each agent e only has access to its local dataset: $D_e = \{(x_e, y_e)\}_{i=1}^{n_e}$, which is sampled from a distribution \mathcal{P}_e . The goal of standard FedAvg training is to minimize the overall loss $\mathcal{L}_E(\theta)$ based on the local loss $\mathcal{L}_e(\theta)$ of each agent:

$$\begin{aligned} \min_{\theta} \mathcal{L}_E(\theta) &= \sum_{e \in [E]} \frac{|D_e|}{n} \mathcal{L}_e(\theta), \\ \mathcal{L}_e(\theta) &= \mathbb{E}_{(x,y) \in \mathcal{P}_e} \ell(h_{\theta}(x), y). \end{aligned} \quad (1)$$

where $\ell(\cdot, \cdot)$ is a loss function given model prediction $h_{\theta}(x)$ and label y (e.g., cross-entropy loss), $n = \sum_{e \in [E]} |D_e|$ represents the total number of training samples, and θ represents the parameter of trained global model.

Intuitively, the performance of agents with high-quality and clean data could be severely compromised by the existence of large amounts of agents with low-quality and noisy data under FedAvg. To solve such a problem and characterize the distinctions of local data distributions (contributions) among agents to ensure fairness, we propose fairness via agent-awareness in FL (FAA) as follows.

Definition 3.1 (Fairness via agent-awareness for FL (FAA)). Given a set of agents E in FL, the overall fairness score among all agents is defined as the maximal difference of excess risks for any pair of agents:

$$\mathcal{FAA}(\{\theta_e\}_{e \in [E]}) = \max_{e_1, e_2 \in [E]} \left| \mathcal{E}_{e_1}(\theta_{e_1}) - \mathcal{E}_{e_2}(\theta_{e_2}) \right|. \quad (2)$$

where θ_e is the local model for agent $e \in [E]$. The excess risk $\mathcal{E}_e(\theta_e)$ for agent e given model θ_e is defined as the difference between the population loss $\mathcal{L}_e(\theta_e)$ and the Bayes optimal error of the corresponding data distribution, i.e.,

$$\mathcal{E}_e(\theta_e) = \mathcal{L}_e(\theta_e) - \min_{\theta^*} \mathcal{L}_e(\theta^*), \quad (3)$$

where θ^* denotes any possible models.

Note that in FedAvg, each client uses the global model θ as its local model θ_e . Definition 3.1 represents a quantitative data-dependent measurement of agent-level fairness. Instead of forcing accuracy parity among all agents regardless of their data quality, we define agent-level fairness as the equity of *excess risks* among agents, which takes the contributions of local data into account by measuring their Bayes errors. For instance, when a local agent has low-quality data, although the corresponding utility loss would be high, the Bayes error of such low-quality data is also high, and thus the excess risk of the user is still low, enabling the agents with high-quality data to achieve low utility loss for fairness. According to the definition, we note that *lower FAA indicates stronger fairness among agents*.

3.2. Fair Federated Learning on Heterogeneous Data via Clustering (FOCUS)

Method Overview. To enhance the fairness of FL in terms of FAA, we provide an agent clustering-based FL algorithm (FOCUS) by partitioning agents conditioned on their data distributions. Intuitively, grouping agents with similar local data distributions and similar contributions together helps to improve fairness, since it reduces the intra-cluster data heterogeneity. We will analyze the fairness achieved by FOCUS and compare it with standard FedAvg both theoretically (Section 4.2) and empirically (Section 5).

Our FOCUS algorithm (Algorithm 1) leverages the Expectation-Maximization algorithm to perform agent clustering. Define M as the number of clusters and E as the number of agents. The goal of FOCUS is to simultaneously optimize the soft clustering labels Π and model weights W . Specifically, $\Pi = \{\pi_{em}\}_{e \in [E], m \in [M]}$ are the dynamic soft clustering labels, representing the estimated probability that agent e belongs to cluster m ; $W = \{w_m\}_{m \in [M]}$ represent the model weights for M data clusters. Given E agents with datasets D_1, \dots, D_E , our FOCUS algorithm follows a two-step scheme that alternately optimizes Π and W .

E step. Expectation steps update the cluster labels Π given the current estimation of (Π, W) . At k -th communication round, the server broadcasts the M cluster models to all agents. The agents calculate the expected training loss $\mathbb{E}_{(x,y) \in D_e} \ell(x, y; w_m^{(t)})$ for each cluster model $w_m^{(t)}$, $m \in [M]$, and then update the soft clustering labels Π according to Equation (8).

M step. The goal of M steps in Equation (9) is to minimize a weighted sum of empirical losses for all local agents. However, given distributed data, it is impossible to find its exact optimal solution in practice. Thus, we specify a concrete protocol in Equation (4) ~ Equation (6) to estimate the objective in Equation (9). At t -th communication round, for each cluster model $w_m^{(t)}$ received from server, each agent e first initializes its local model $\theta_{em(0)}^{(t)}$ as $w_m^{(t)}$, and then

Algorithm 1 EM clustered federated learning algorithm

Input: Agents with data $\{D_i\}_{i \in [E]}$ and M learning models. Initialize weights $w_m^{(0)}$ and $\pi_{em}^{(0)} = \frac{1}{M}$ for $m \in [M]$ and $e \in [E]$.

for $t = 0$ to $T - 1$ **do**

for agent $e \in [E]$ **do**

for model $m \in [M]$ **do**

 E step:

$$\pi_{em}^{(t+1)} \leftarrow \frac{\pi_{em}^{(t)} \exp\left(-\mathbb{E}_{(x,y) \in D_e} \ell(x, y; w_m^{(t)})\right)}{\sum_{m=1}^M \pi_{em}^{(t)} \exp\left(-\mathbb{E}_{(x,y) \in D_e} \ell(x, y; w_m^{(t)})\right)} \quad (8)$$

end for

end for

for model $m \in [M]$ **do**

 M step:

$$w_m^{(t+1)} \leftarrow \arg \min_w \sum_{e=1}^E \pi_{em}^{(t+1)} \sum_{i=1}^{n_e} \ell\left(h_w(x_e^{(i)}), y_e^{(i)}\right) \quad (9)$$

end for

end for

Return model weights $w_m^{(T)}$

updates the model using its own dataset. To reduce communication costs, each agent is allowed to run SGD locally for K local steps as shown in Equation (5). After K local steps, each agent sends the updated models $\theta_{em(K)}^{(t)}$ back to the central server, and the server aggregates the models of all agents by a weighted average based on the soft clustering labels $\{\pi_{em}\}$. We provide theoretical analysis for the convergence and optimality of FOCUS under these multiple local updates in Section 4.

Clients: $\theta_{em(0)}^{(t)} = w_m^{(t)}$. (4)

$$\theta_{em(k+1)}^{(t)} = \theta_{em(k)}^{(t)} - \eta_k \nabla \sum_{i=1}^{n_e} \ell\left(h_{\theta_{em(k)}^{(t)}}(x_e^{(i)}), y_e^{(i)}\right), \quad \forall k = 1, \dots, K - 1. \quad (5)$$

Server: $w_m^{(t+1)} = \sum_{e=1}^E \frac{\pi_{em}^{(t+1)} \theta_{em(K)}^{(t)}}{\sum_{e'=1}^E \pi_{e'm}^{(t+1)}}.$ (6)

Inference. At inference time, each agent ensembles the M models by a weighted average on their prediction probabilities, i.e., a agent e predicts $\sum_{m=1}^M \pi_{em} h_{w_m}(x)$ for input x . Suppose a test dataset D_e^{test} is sampled from distribution \mathcal{P}_e . The test loss can be calculated by

$$\mathcal{L}_{test}(W, \Pi) = \frac{1}{|D_e^{test}|} \sum_{(x,y) \in D_e^{test}} \ell\left(\sum_{m=1}^M \pi_{em} h_w(x), y\right) \quad (7)$$

For unseen agents that do not participate in the training process, their clustering labels Π are unknown. Therefore, an unseen agent e computes its one-shot clustering label $\pi_{em}^{(1)}$, $m \in [M]$ according to Equation (8), and outputs predictions $\sum_{m=1}^M \pi_{em}^{(1)} h_{w_m}(x)$ for the test sample x .

4. Theoretical Analysis of FOCUS

In this section, we first present the convergence and optimality guarantees of our FOCUS algorithm; and then prove

that it improves the fairness of FL regarding FAA. Our analysis considers linear models and then extends to nonlinear models with smooth and strongly convex loss functions.

4.1. Convergence Analysis

Linear models. We first start with linear models to deliver the main idea of our analysis. Suppose there are E agents, each with a local dataset $D_e = \{(x_e^{(i)}, y_e^{(i)})\}_{i=1}^{n_e}$, ($e \in [E]$) generated from a Gaussian distribution. Specifically, we assume each dataset D_e has a mean vector $\mu_e \in \mathbb{R}^d$, and $(x_e^{(i)}, y_e^{(i)})$ is generated by $y_e^{(i)} = \mu_e^T x_e^{(i)} + \epsilon_e^{(i)}$, where $x_e^{(i)}$ is a random vector $x_e^{(i)} \sim \mathcal{N}(0, \delta^2 I_d)$ and the label $y_e^{(i)}$ is perturbed by some random noise $\epsilon_e^{(i)} \sim \mathcal{N}(0, \sigma^2)$. Each agent is asked to minimize the mean squared error to estimate μ_e , so the empirical loss function for a local agent given D_e is

$$\mathcal{L}_{emp}(D_e; w) = \frac{1}{n_e} \sum_{i=1}^{n_e} (w^T x_e^{(i)} - y_e^{(i)})^2. \quad (10)$$

We further make the following assumption about the heterogeneous agents.

Assumption 4.1 (Separable distributions). Suppose there are M predefined vectors $\{w_i^*\}_{i=1}^M$, where for any $m_1, m_2 \in [M]$, $m_1 \neq m_2$, $\|w_{m_1}^* - w_{m_2}^*\|_2 \geq R$. A set of agents E satisfy separable distributions if they can be partitioned into M subsets S_1, \dots, S_M such that, for any agent $e \in S_m$, $\|\mu_e - w_m^*\|_2 \leq r < \frac{R}{2}$.

Assumption 4.1 guarantees that the heterogeneous local data distributions are separable so that an optimal clustering solution exists, in which $\{w_1^*, \dots, w_M^*\}$ are the centers of clusters.

We next present Theorem 4.2 to demonstrate the linear convergence rate to the optimal cluster centers for FOCUS. Detailed proofs can be found in Appendix B.1.

Theorem 4.2. Assume the agent set E satisfies the separable distributions condition in Assumption 4.1. Given trained M models with $\pi_{em}^{(0)} = \frac{1}{M}$, $\forall e, m$. Under the natural initialization w_m for each model $m \in [M]$, which satisfies $\exists \Delta_0 > 0$, $\|w_m^{(0)} - w_m^*\|_2 \leq \min_{m' \neq m} \|w_m^{(0)} - w_{m'}^*\|_2 - 2(r + \Delta_0)$ and $|D_e| = O(d)$. If learning rate $\eta \leq \min(\frac{1}{4\delta^2}, \frac{\beta}{\sqrt{T}})$, FOCUS converges by

$$\pi_{em}^{(T)} \geq \frac{1}{1 + (M-1) \cdot \exp(-2R\delta^2 \Delta_0 T)}, \forall e \in S_m \quad (11)$$

$$\mathbb{E}\|w_m^{(T)} - w_m^*\|_2^2 \leq \left(1 - \frac{2\eta\gamma_m\delta^2}{M}\right)^{KT} (\|w_m^{(0)} - w_m^*\|_2^2 + A) + 2MKr + \frac{1}{2}M\delta^2 E\beta T^{-1/2} O(K^3, \sigma^2). \quad (12)$$

where T is the total number of communication rounds; K is the number of local updates in each communication round; $\gamma_m = |S_m|$ is the number of agents in the m -th cluster, and

$$A = \frac{2EK(M-1)\delta^2}{\left(1 - \frac{2\eta\delta^2\gamma_m}{M}\right)^K - \exp(-2R\delta^2\Delta_0)}.$$

(caused by initial inaccurate clustering)

Proof sketch. To prove this theorem, we first consider E steps and M steps separately to derive corresponding convergence lemmas (Lemmas B.1 and B.2). In E steps, the soft cluster labels π_{em} increase for all $e \in S_m$, as long as $\|w_m^{(t)} - w_m^*\|_2 < \|w_{m'}^{(t)} - w_m^*\|_2, \forall m' \neq m$. On the other hand, $\|w_m^{(t)} - w_m^*\|$ is guaranteed to shrink linearly as long as π_{em} is large enough for any $e \in S_m$. We then integrate Lemmas B.1 and B.2 and prove Theorem 4.2 using an induction argument. \square

Remarks. Theorem 4.2 shows the convergence of parameters (Π, W) to a near-optimal solution. Equation (11) implies that the agents will be *correctly clustered* since π_{em} will converge to 1 as the number of communication rounds K increases. In Equation (12), the first term diminishes exponentially, while the second term $2MKr$ reflects the intra-cluster distribution divergence r . The last term originates from the data heterogeneity among clients across different clusters. Its influence is amplified by the number of local updates ($O(K^3)$) and will also diminish to zero as the number of communication rounds T goes to infinity. Our convergence analysis is conditioned on the natural clustering initialization for model weights $w_m^{(0)}$ towards a corresponding cluster center w_m^* , which is standard in convergence analysis for a mixture of models (Yan et al., 2017; Balakrishnan et al., 2017).

Smooth and strongly convex loss functions. Next, we extend our analysis to a more general case of non-linear models with L -smooth and μ -strongly convex loss function.

Assumption 4.3 (Smooth and strongly convex loss functions). The population loss functions $\mathcal{L}_e(\theta)$ for each agent e is L -smooth, i.e., $\|\nabla^2 \mathcal{L}_e(\theta)\|_2 \leq L$. The loss functions are μ -strongly convex, if the eigenvalues λ of the Hessian matrix $\nabla^2 \mathcal{L}_e(\theta)$ satisfy $\lambda_{\min}(\nabla^2 \mathcal{L}_e(\theta)) \geq \mu$.

We further make an assumption similar to Assumption 4.1 for the general case:

Assumption 4.4 (Separable distributions). A set of agents E satisfy separable distributions if they can be partitioned into M subsets S_1, \dots, S_M with w_1^*, \dots, w_M^* representing the center of each set respectively, and the optimal parameter θ^* of each local loss \mathcal{L}_e (i.e., $\theta_e^* = \arg \min_{\theta} \mathcal{L}_e(\theta)$) satisfy $\|\theta_e^* - w_m^*\|_2 \leq r$. In the meantime, agents from different subsets have different data distributions, such that $\|w_{m_1}^* - w_{m_2}^*\|_2 \geq R, \forall m_1, m_2 \in [M], m_1 \neq m_2$.

Theorem 4.5. Assume the agent set E satisfies the separable distributions condition in Assumption 4.4. Suppose loss functions have bounded variance for gradients on local

datasets, i.e., $\mathbb{E}_{(x,y) \sim \mathcal{D}_e} [\|\nabla \ell(x, y; \theta) - \nabla \mathcal{L}_e(\theta)\|_2^2] \leq \sigma^2$, and the population losses are bounded, i.e., $\mathcal{L}_e \leq G, \forall e \in [E]$. With $\pi_{em}^{(0)} = \frac{1}{M}, \exists \Delta_0 > 0, \|w_m^{(0)} - w_m^*\|_2 \leq \frac{\sqrt{\mu}R}{\sqrt{\mu} + \sqrt{L}} - r - \Delta_0$, and the learning rate of each agent $\eta \leq \min(\frac{1}{2(\mu+L)}, \frac{\beta}{\sqrt{T}})$, FOCUS converges by

$$\pi_{em}^{(T)} \geq \frac{1}{1 + (M-1) \exp(-\mu R \Delta_0 T)}, \forall e \in S_m \quad (13)$$

$$\mathbb{E} \|w_m^{(T)} - w_m^*\|_2^2 \leq (1 - \eta A)^{KT} (\|w_m^{(0)} - w_m^*\|_2^2 + B) + O(Kr) + ME\beta O(K^3, \frac{\sigma^2}{ne}) T^{-1/2} \quad (14)$$

where T is the total number of communication rounds; K is the number of local updates in each communication round; $\gamma_m = |S_m|$ is the number of agents in the m -th cluster, and

$$A = \underbrace{\frac{2\gamma_m}{M} \frac{\mu L}{\mu + L}}_{\text{related to convergence rate}}, B = \underbrace{\frac{GMT E (\frac{4L}{\mu} + \frac{6}{\mu(\mu+L)})}{(1 - \eta A)^K - \exp(-\mu R \Delta_0)}}_{\text{caused by the offset of initial clustering}}. \quad (15)$$

Proof sketch. We analyze the evolution of parameters (Π, W) for E steps in Lemma B.3 and M steps in Lemma B.4. Lemma B.3 shows that the soft cluster labels π_{em} increase for all $e \in S_m$ in E steps as long as $\|w_m - w_m^*\|_2 < \frac{\sqrt{\mu}R}{\sqrt{\mu} + \sqrt{L}} - r$; whereas Lemma B.4 guarantees that the model weights w_m get closer to the optimal solution w_m^* in M steps. We combine Lemmas B.3 and B.4 by induction to prove this theorem. Detailed proofs are deferred to Appendix B.2.3. \square

Remarks. Theorem 4.5 extends the convergence guarantee of (Π, W) from linear models (Theorem 4.2) to general models with smooth and convex loss functions. For any agent e that belongs to a cluster m ($e \in S_m$), its soft cluster label π_{em} converges to 1 based on Equation (13), indicating the clustering optimality. Meanwhile, the model weights W converge linearly to a near-optimal solution. The error term $O(Kr)$ in Equation (14) is expected since r represents the data divergence within each cluster and w_m^* denotes the center of each cluster. The last term in Equation (14) implies a trade-off between communication cost and convergence speed. Increasing K reduces communication cost by $O(\frac{1}{K})$ but at the expense of slowing down the convergence.

4.2. Fairness Analysis

To theoretically show that FOCUS achieves stronger fairness in FL based on FAA, here we focus on a simple yet representative case where all agents share similar distributions except one outlier agent.

Linear models. We first concretize such a scenario for linear models. Suppose we have E agents learning weights for M linear models. Their local data $D_e(e \in [E])$ are generated by $y_e^{(i)} = \mu_e^T x_e^{(i)} - \epsilon_e^{(i)}$ with $x_e^{(i)} \sim \mathcal{N}(0, \delta^2 I_d)$ and $\epsilon_e^{(i)} \sim \mathcal{N}(0, \sigma_e^2)$. $E - 1$ agents learn from a normal dataset

with ground truth vector μ_1, \dots, μ_{E-1} and $\|\mu_e - \mu^*\|_2 \leq r$, while the E -th agent has an outlier data distribution, with its the ground truth vector μ_E far away from other agents, i.e., $\|\mu_E - \mu^*\|_2 \geq R$.

As stated in Theorem 4.2, the soft clustering labels and model weights (Π, W) converge linearly to the global optimum. Therefore, we analyze the fairness of FOCUS, assuming an optimal (Π, W) is reached. We compare the FAA achieved by FOCUS and FedAvg to underscore how our algorithm helps improve fairness for heterogeneous agents.

Theorem 4.6. *When a single agent has an outlier distribution, the fairness FAA achieved by FOCUS algorithm with two clusters $M = 2$ is*

$$\mathcal{FAA}_{focus}(W, \Pi) \leq \delta^2 r^2. \quad (16)$$

while the fairness FAA achieved by FedAvg is

$$\mathcal{FAA}_{avg}(W) \geq \delta^2 \left(\frac{R^2(E-2) - 2Rr}{E} + r^2 \right) = \Omega(\delta^2 R^2). \quad (17)$$

Remarks. When a single outlier exists, the fairness gap between Fedavg and FOCUS is shown by Theorem 4.6.

$$\mathcal{FAA}_{avg}(W) - \mathcal{FAA}_{focus}(W, \Pi) \geq \delta^2 \left(\frac{R^2(E-2) - 2Rr}{E} \right). \quad (18)$$

As long as $R > \frac{2r}{E-2}$, FOCUS is guaranteed to achieve stronger fairness (i.e., lower FAA) than FedAvg. Note that *the outlier assumption only makes sense when $E > 2$* since one cannot tell which agent is the outlier when $E = 2$. Also, we naturally assume $R > 2r$ so that the two underlying clusters are at least separable. Therefore, we conclude that FOCUS dominates than FedAvg in terms of FAA. Here we only discuss the scenario of a single outlier agent for clarity, but similar conclusions can be drawn for multiple underlying clusters and $M > 2$, as discussed in Appendix C.1.

Smooth and strongly convex loss functions. We generalize the fairness analysis to nonlinear models with smooth and convex loss functions. To illustrate the superiority of our FOCUS algorithms in terms of FAA fairness, we similarly consider training in the presence of an outlier agent. Suppose we have E agents that learn weights for M models. We assume their population loss functions are L -smooth, μ -strongly convex (as in Assumption 4.3) and bounded, i.e., $\mathcal{L}_e(\theta) \leq G$. $E - 1$ agents learn from similar data distributions, such that the total variation distance between the distributions of any two different agents $i, j \in [E - 1]$ is no greater than r : $D_{TV}(\mathcal{P}_i, \mathcal{P}_j) \leq r$. On the other hand, the E -th agent has an outlier data distribution, such that the Bayes error $\mathcal{L}_E(\theta_i^*) - \mathcal{L}_E(\theta_E^*) \geq R$ for any $i \in [E - 1]$. We claim that this assumption can be reduced to a lower bound on H-divergence (Zhao et al., 2022) between distributions \mathcal{P}_i and \mathcal{P}_E that $D_H(\mathcal{P}_i, \mathcal{P}_E) \geq \frac{LR}{4\mu}$. (See proofs in Appendix C.3.)

Theorem 4.7. *The fairness FAA achieved by FOCUS with two clusters $M = 2$ is*

$$\mathcal{FAA}_{focus}(W, \Pi) \leq \frac{2Gr}{E-1} \quad (19)$$

Let $B = \frac{2Gr}{E-1}$. The fairness achieved by FedAvg is

$$\begin{aligned} \mathcal{FAA}_{avg}(W) \geq & \left(\frac{E-1}{E} - \frac{L}{\mu E^2} \right) R - \left(1 + \frac{L(E-1)}{\mu E} - \frac{L^2}{\mu^2 E} \right) B \\ & - \frac{2L}{\mu E} \sqrt{B \left(R - \frac{L}{\mu} B \right)} \quad (20) \end{aligned}$$

Remarks. Notably, when the outlier distribution is very different from the normal distribution, such that $R \gg Gr$ (which means $B \ll R$), we simplify Equation (20) as

$$\mathcal{FAA}_{avg}(W) \geq \left(\frac{E-1}{E} - \frac{L}{\mu E^2} \right) R.$$

Note that $\mathcal{FAA}_{focus}(W, \Pi) \leq B \ll R$, so the fairness FAA achieved by FedAvg is always larger (weaker) than that of FOCUS, as long as $E \geq \sqrt{L/\mu}$, indicating the effectiveness of FOCUS.

5. Experimental Evaluation

We conduct extensive experiments on various heterogeneous data settings to evaluate the fairness measured by FAA for FOCUS, FedAvg (McMahan et al., 2017), and two baseline fair FL algorithms (i.e., q-FFL (Li et al., 2020b) and AFL (Mohri et al., 2019)). We show that FOCUS achieves significantly higher fairness measured by FAA while maintaining similar or even higher accuracy.

5.1. Experimental Setup

Data and Models. We carry out experiments on four different datasets with heterogeneous data settings, ranging from synthetic data for linear models to images (rotated MNIST (Deng, 2012) and rotated CIFAR (Krizhevsky, 2009)) to text data for sentiment classification on Yelp (Zhang et al., 2015) and IMDB (Maas et al., 2011) datasets. We train a fully connected model consisting of two linear layers with ReLU activations for MNIST, a ResNet 18 model (He et al., 2016) for CIFAR, and a pre-trained BERT-base model (Devlin et al., 2019) for the text data. We refer the readers to Appendix A.1 for more implementation details.

Evaluation Metrics and Implementation Details. We consider three evaluation metrics: average test accuracy, average test loss, FAA for fairness, and the existing fairness metric ‘‘agnostic loss’’ introduced by (Mohri et al., 2019). For FedAvg, we evaluate the trained global model on each agent’s test data; for FOCUS, we train M models corresponding to M clusters, and use the soft clustering labels $\Pi = \{\pi_{em}\}_{e \in [E], m \in [M]}$ to make aggregated predictions on each agent’s test data. We also report the performance of existing fair FL algorithms (i.e., q-FFL (Li et al.,

Table 1: Comparison of FOCUS, FedAvg, and fair FL algorithms q-FFL, AFL, Ditto and CGSV, in terms of average test accuracy (Avg Acc), average test loss (Avg Loss), fairness FAA and existing fairness metric Agnostic loss. FOCUS achieves the best fairness measured by FAA compared with all baselines.

		FOCUS	FedAvg	q-FFL			AFL	Ditto	CGSV
				$q = 0.1$	$q = 1$	$q = 10$			
Synthetic	Avg Loss	0.010	0.108	0.106	0.102	0.110	0.104	0.023	0.260
	FAA	0.001	0.958	0.769	0.717	0.699	0.780	0.012	0.010
Rotated MNIST	Avg Acc	0.953	0.929	0.922	0.861	0.685	0.885	0.940	0.938
	Avg Loss	0.152	0.246	0.269	0.489	1.084	0.429	0.210	0.222
	FAA	0.094	0.363	0.388	0.612	0.253	0.220	0.104	0.210
	Agnostic Loss	0.224	0.616	0.656	1.018	1.271	0.548	0.354	0.331
Rotated CIFAR	Avg Acc	0.688	0.654	0.648	0.592	0.121	0.661	0.657	0.515
	Avg Loss	1.133	2.386	1.138	1.141	2.526	1.666	2.382	3.841
	FAA	0.360	1.115	0.620	0.473	0.379	0.595	0.758	1.317
	Agnostic Loss	1.294	3.275	1.610	1.439	2.526	2.179	3.053	3.841
Yelp/IMDb	Avg Acc	0.940	0.940	0.938	0.938	0.909	0.934	0.933	0.701
	Avg Loss	0.174	0.236	0.188	0.179	0.264	0.187	0.191	0.547
	FAA	0.047	0.098	0.052	0.051	0.070	0.049	0.049	0.462
	Agnostic Loss	0.257	0.349	0.266	0.253	0.242	0.253	0.263	0.700

2020b), AFL (Mohri et al., 2019), Ditto (Li et al., 2021), and CGSV (Xu et al., 2021)) as well as existing state-of-the-art FL algorithms in heterogeneous data settings (i.e., FedMA (Wang et al., 2020), Bayesian nonparametric FL (Yurochkin et al., 2019) and FedProx (Li et al., 2020a) in Appendices A.2 and A.3).

To evaluate FAA of different algorithms, we estimate the Bayes optimal loss $\min_w \mathcal{L}_e(w)$ for each local agent e . Specifically, we train a centralized model based on the subset of agents with similar data distributions (i.e., the same ground-truth cluster) and use it as a *surrogate* to approximate the Bayes optimum. We select the agent pair with the maximal difference of excess risks to measure fairness in terms of FAA calculated following Definition 3.1.

5.2. Evaluation Results

Synthetic data for linear models. We first evaluate FOCUS on linear regression models with synthetic datasets. We fix $E = 10$ agents with data sampled from Gaussian distributions. Each agent e is assigned with a local dataset of $D_e = \{(x_e^{(i)}, y_e^{(i)})\}_{i=1}^{n_e}$ generated by $y_e^{(i)} = \mu_e^T x_e^{(i)} + \epsilon_e^{(i)}$ with $x_e^{(i)} \sim \mathcal{N}(0, I_d)$ and $\epsilon_e^{(i)} \sim \mathcal{N}(0, \sigma^2)$. We study the case considered in Section 4.2 where a single agent has an outlier data distribution. We set the intra-cluster distance $r = 0.01$ and the inter-cluster distance $R = 1$ in our experiment. Note that it is a regression task, so we mainly report the average test loss instead of accuracy here. Table 1 shows that FOCUS achieves FAA of 0.001, much lower than the 0.958 achieved by FedAvg, 0.699 by q-FFL, and 0.780 by AFL.

Rotated MNIST and CIFAR. Following (Ghosh et al., 2020), we rotate the images MNIST and CIFAR datasets with different degrees to create data heterogeneity among agents. Both datasets are evenly split into 10 subsets for

10 agents. For MNIST, two subsets are rotated for 90 degrees, one subset is rotated for 180 degrees, and the rest seven subsets are unchanged, yielding an FL setup with three ground-truth clusters. Similarly, for CIFAR, we fix the images of 7 subsets and rotate the other 3 subsets for 180 degrees, thus creating two ground-truth clusters. From Table 1, we observe that FOCUS consistently achieves higher average test accuracy, lower average test loss, and lower FAA than other methods on both datasets. In addition, although existing fair algorithms q-FFL and AFL achieve lower FAA scores than FedAvg, their average test accuracy drops significantly. This is mainly because these fair algorithms are designed for performance parity via improving low-quality agents (i.e., agents with high training loss), thus sacrificing the accuracy of high-quality agents. In contrast, FOCUS improves both the FAA fairness and preserves high test accuracy.

Next, we analyze the surrogate excess risk of every agent on MNIST in Figure 1 (a). We observe that the global model trained by FedAvg obtains the highest test loss as 0.61 on the outlier cluster, which rotates 180 degrees (i.e., cluster C3), resulting in high excess risk for the 9th agent. Moreover, the low-quality data of the outlier cluster affect the agents in the 1st cluster via FedAvg training, which leads to a much higher excess risk than that of FOCUS. On the other hand, FOCUS successfully identifies clusters of the outlier distributions, i.e., clusters 2 and 3, rendering models trained from the outlier clusters independent from the normal cluster 1. As shown in Figure 1, our FOCUS reduces the excess risks of all agents, especially the outliers, on different datasets. This leads to strong fairness among agents in terms of FAA. Similar trends are also observed in CIFAR, in which our FOCUS reduces the surrogate excess risk for the 9th agent from 2.74 to 0.44. We omit the loss

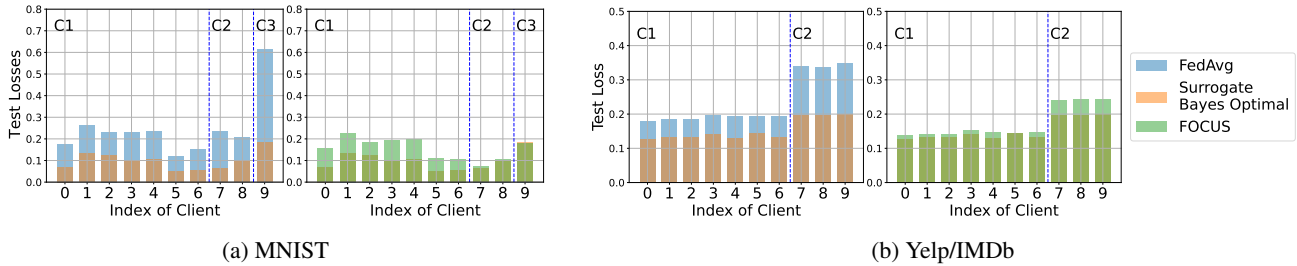


Figure 1: The excess risks of different agents trained with FedAvg and FOCUS on MNIST (a) and Yelp/IMDb text data (b). C_i denotes i th cluster.

histogram of CIFAR to Appendix A.9.

Table 2: Comparison of FOCUS and FedAvg with different numbers of outlier agents (k) in terms of average test accuracy (Avg Acc) and fairness FAA.

		Rotated MNIST			Rotated CIFAR		
		$k = 1$	$k = 3$	$k = 5$	$k = 1$	$k = 3$	$k = 5$
Avg Acc	FOCUS	0.957	0.953	0.948	0.683	0.688	0.677
	FedAvg	0.945	0.929	0.910	0.683	0.654	0.651
FAA	FOCUS	0.159	0.094	0.153	1.168	0.360	0.436
	FedAvg	0.515	0.363	0.476	2.464	1.115	1.166

Additionally, we evaluate different numbers of outliers in Table 2. In the presence of 1, 3, and 5 outlier agents, forming 2, 3, or 4 underlying true clusters, FOCUS consistently achieves a lower FAA score and higher accuracy.

In practice, we do not know the number of underlying clusters, so we set $M = 2, 3, 4$ while we have 3 true underlying clusters in Table 3 on MNIST. It shows that when $M = 2, 3, 4$, FOCUS achieves similar accuracy and fairness. When $M = 1$, FOCUS reduces to FedAvg, leading to the worst accuracy and fairness under heterogeneous data. A similar trend also occurs for CIFAR, as shown in Table 3.

Table 3: The effect of the predefined number M on Rotate MNIST with 3 underlying clusters and on Rotated CIFAR with 2 underlying clusters.

		Rotated MNIST				Rotated CIFAR			
		$M = 1$	$M = 2$	$M = 3$	$M = 4$	$M = 1$	$M = 2$	$M = 3$	$M = 4$
Avg Acc	0.929	0.952	0.953	0.953	0.654	0.688	0.696	0.693	
Avg loss	0.246	0.167	0.152	0.153	2.386	1.133	0.932	0.921	
FAA	0.363	0.079	0.094	0.091	1.115	0.360	0.323	0.350	
Agnostic	0.616	0.272	0.224	0.223	3.275	1.294	1.115	1.098	

Sentiment classification. We evaluate FOCUS on the sentiment classification task with text data, Yelp (restaurant reviews), and IMDb (movie reviews), which naturally form data heterogeneity among 10 agents and thus create 2 clusters. Specifically, we sample 56k reviews from Yelp datasets distributed among seven agents and use the whole 25k IMDB datasets distributed among three agents to simulate the heterogeneous setting. From Table 1, we can see that while the average test accuracy of FOCUS, FedAvg, and other fair FL algorithms are similar, FOCUS achieves a lower average test loss. In addition, the FAA of FOCUS is significantly lower than other baselines, indicating stronger fairness. We also observe from Figure 1 (b) that the ex-

cess risk of FOCUS on the outlier cluster (i.e., C2) drops significantly compared with that of FedAvg.

Ablation Studies. To provide a more comprehensive evaluation for FOCUS, we present additional ablation studies on scalability, convergence rate, and runtime analysis. Figure 2 is a comparison of the convergence rate of different methods on rotated MNIST, which shows that FOCUS converges faster and achieves better performance on MNIST under a large number of clients. Additional results in Appendices A.4 to A.6 show that FOCUS is scalable to larger client groups and consumes comparable running time with other methods on different datasets. Moreover, we compare FOCUS to a cluster-wise FedAvg algorithm with hard clustering, illustrating the advantages of FOCUS using soft-clustering when the underlying clusters are not perfectly separable. We refer readers to Appendix A.7 for further discussions.

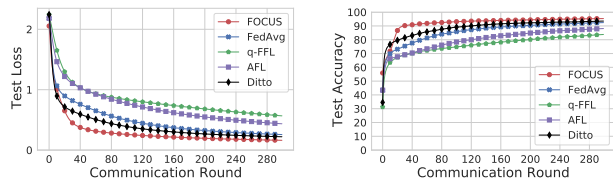


Figure 2: Comparison of the convergence rate of different methods on rotated MNIST with 100 clients.

6. Conclusion

In this work, we provide an agent-level fairness measurement in FL (FAA) by taking agents’ inherent heterogeneous data properties into account. Motivated by our fairness definition in FL, we also provide an effective FL training algorithm FOCUS to achieve high fairness. We theoretically analyze the convergence rate and optimality of FOCUS, and we prove that under mild conditions, FOCUS is always fairer than the standard FedAvg protocol. We conduct thorough experiments on synthetic data with linear models as well as image and text datasets on deep neural networks. We show that FOCUS achieves stronger fairness than FedAvg and achieves similar or higher prediction accuracy across all datasets. We believe our work will inspire new research efforts on exploring the suitable fairness measurements for FL under different requirements.

References

- Adnan, M., Kalra, S., Cresswell, J., Taylor, G., and Tizhoosh, H. Federated learning and differential privacy for medical image analysis. volume 12, 02 2022. doi: 10.1038/s41598-022-05539-7.
- Alawadi, S., Victor R. KEBANDE, Y. D., Bugeja, J., Persson, J. A., and Olsson, C. M. A federated interactive learning iot-based health monitoring platform. In *European Conference on Advances in Databases and Information Systems*, pp. 235–246, 2021. URL <http://www.diva-portal.org/smash/get/diva2:1584574/FULLTEXT01.pdf>.
- Anelli, V. W., Deldjoo, Y., Tommaso Di Noia, A. F., and Narducci, F. Federated recommender systems with learning to rank. In *29-th Italian Symposium on Advanced Database Systems (SEBD)*, 2021. URL <https://sisinflab.poliba.it/publications/2021/ADDFN21b/paper7.pdf>.
- Balakrishnan, S., Wainwright, M. J., and Yu, B. Statistical guarantees for the em algorithm: From population to sample-based analysis. *The Annals of Statistics*, 45(1): 77–120, 2017.
- Buolamwini, J. and Gebru, T. Gender shades: Intersectional accuracy disparities in commercial gender classification. In *Conference on fairness, accountability and transparency*, pp. 77–91. PMLR, 2018.
- Chu, L., Wang, L., Dong, Y., Pei, J., Zhou, Z., and Zhang, Y. Fedfair: Training fair models in cross-silo federated learning. 2021. URL <https://arxiv.org/pdf/2109.05662.pdf>.
- Deng, L. The mnist database of handwritten digit images for machine learning research. *IEEE Signal Processing Magazine*, 29(6):141–142, 2012.
- Devlin, J., Chang, M.-W., Lee, K., and Toutanova, K. Bert: Pre-training of deep bidirectional transformers for language understanding. In *Proceedings of the 2019 Conference of the North American Chapter of the Association for Computational Linguistics: Human Language Technologies, Volume 1 (Long and Short Papers)*, pp. 4171–4186, 2019.
- Donahue, K. and Kleinberg, J. Models of fairness in federated learning. 2022a. URL <https://arxiv.org/pdf/2112.00818.pdf>.
- Donahue, K. and Kleinberg, J. Models of fairness in federated learning. 2022b. URL <https://arxiv.org/abs/2112.00818>.
- Dwork, C., Hardt, M., Pitassi, T., Reingold, O., and Zemel, R. Fairness through awareness. In *Proceedings of the 3rd innovations in theoretical computer science conference*, pp. 214–226, 2012.
- Ghosh, A., Chung, J., Yin, D., and Ramchandran, K. An efficient framework for clustered federated learning. *Advances in Neural Information Processing Systems*, 33: 19586–19597, 2020.
- Hard, A., Rao, K., Mathews, R., Ramaswamy, S., Beaufays, F., Augenstein, S., Eichner, H., Kiddon, C., and Ramage, D. Federated learning for mobile keyboard prediction. *arXiv preprint arXiv:1811.03604*, 2018.
- Hardt, M., Price, E., and Srebro, N. Equality of opportunity in supervised learning. *Advances in neural information processing systems*, 29, 2016.
- He, K., Zhang, X., Ren, S., and Sun, J. Deep residual learning for image recognition. In *Proceedings of the IEEE Conference on Computer Vision and Pattern Recognition (CVPR)*, June 2016.
- Hu, S., Wu, Z. S., and Smith, V. Provably fair federated learning via bounded group loss. 2022. URL <https://arxiv.org/pdf/2203.10190.pdf>.
- Kang, J., Xiong, Z., Niyato, D., Yu, H., Liang, Y.-C., and Kim, D. I. Incentive design for efficient federated learning in mobile networks: A contract theory approach. 2019. URL <https://arxiv.org/pdf/1905.07479.pdf>.
- Krizhevsky, A. Learning multiple layers of features from tiny images. Technical report, 2009.
- Li, C., Li, G., and Varshney, P. K. Federated learning with soft clustering. 2022. URL <https://ieeexplore.ieee.org/stamp/stamp.jsp?tp=&arnumber=9174890>.
- Li, T., Sahu, A. K., Zaheer, M., Sanjabi, M., Talwalkar, A., and Smith, V. Federated optimization in heterogeneous networks. *Proceedings of Machine Learning and Systems*, 2:429–450, 2020a.
- Li, T., Sanjabi, M., Beirami, A., and Smith, V. Fair resource allocation in federated learning. In *8th International Conference on Learning Representations, ICLR 2020, Addis Ababa, Ethiopia, April 26-30, 2020*. OpenReview.net, 2020b. URL <https://openreview.net/forum?id=ByexElSYDr>.
- Li, T., Hu, S., Beirami, A., and Smith, V. Ditto: Fair and robust federated learning through personalization. In *International Conference on Machine Learning*, pp. 6357–6368. PMLR, 2021.

- Lim, W. Y. B., Luong, N. C., Hoang, D. T., Jiao, Y., Liang, Y.-C., Yang, Q., Niyato, D., and Miao, C. Federated learning in mobile edge networks: A comprehensive survey. *IEEE Communications Surveys & Tutorials*, 22(3): 2031–2063, 2020.
- Maas, A. L., Daly, R. E., Pham, P. T., Huang, D., Ng, A. Y., and Potts, C. Learning word vectors for sentiment analysis. In *Proceedings of the 49th Annual Meeting of the Association for Computational Linguistics: Human Language Technologies*, pp. 142–150, Portland, Oregon, USA, June 2011. Association for Computational Linguistics. URL <http://www.aclweb.org/anthology/P11-1015>.
- Marfoq, O., Neglia, G., Bellet, A., Kameni, L., and Vidal, R. Federated multi-task learning under a mixture of distributions. In Beygelzimer, A., Dauphin, Y., Liang, P., and Vaughan, J. W. (eds.), *Advances in Neural Information Processing Systems*, 2021. URL <https://openreview.net/forum?id=YCqx6zhEzRp>.
- McMahan, H. B., Moore, E., Ramage, D., Hampson, S., and Agüera y Arcas, B. Communication-efficient learning of deep networks from decentralized data. 2017.
- Minto, L., Haller, M., Haddadi, H., and Livshits, B. Stronger privacy for federated collaborative filtering with implicit feedback. In *Fifteenth ACM Conference on Recommender Systems*, pp. 342–350, 2021. URL <https://doi.org/10.1145/3460231.3474262>.
- Mohri, M., Sivek, G., and Suresh, A. T. Agnostic federated learning. 2019. URL <http://proceedings.mlr.press/v97/mohri19a/mohri19a.pdf>.
- Opper, M. and Haussler, D. Generalization performance of bayes optimal classification algorithm for learning a perceptron. *Physical Review Letters*, 66(20):2677, 1991.
- Ruan, Y. and Joe-Wong, C. Fedsoft: Soft clustered federated learning with proximal local updating. 2022. URL <https://arxiv.org/pdf/2112.06053.pdf>.
- Sattler, F., Müller, K.-R., and Samek, W. Clustered federated learning: Model-agnostic distributed multitask optimization under privacy constraints. 2021. URL <https://ieeexplore.ieee.org/stamp/stamp.jsp?tp=&arnumber=9174890>.
- Sheller, M., Edwards, B., Reina, G., Martin, J., Pati, S., Kotrotsou, A., Milchenko, M., Xu, W., Marcus, D., Colen, R., and Bakas, S. Federated learning in medicine: Facilitating multi-institutional collaboration without sharing patient data. In *Scientific Reports 10*, 2020. URL <https://doi.org/10.1038/s41598-020-69250-1>.
- Stallmann, M. and Wilbik, A. Towards federated clustering: A federated fuzzy c-means algorithm (ffcm). 2022. URL <https://arxiv.org/pdf/2201.07316.pdf>.
- Wang, H., Yurochkin, M., Sun, Y., Papailiopoulos, D., and Khazaeni, Y. Federated learning with matched averaging. *arXiv preprint arXiv:2002.06440*, 2020.
- Wang, Z., Fan, X., Qi, J., Wen, C., Wang, C., and Yu, R. Federated learning with fair averaging. 2021. URL <https://www.ijcai.org/proceedings/2021/0223.pdf>.
- Xie, M., Long, G., Shen, T., Zhou, T., Wang, X., Jiang, J., and Zhang, C. Multi-center federated learning. 2021. URL <https://arxiv.org/abs/2005.01026>.
- Xu, X., Lyu, L., Ma, X., Miao, C., Foo, C. S., and Low, B. K. H. Gradient driven rewards to guarantee fairness in collaborative machine learning. *Advances in Neural Information Processing Systems*, 34:16104–16117, 2021.
- Yan, B., Yin, M., and Sarkar, P. Convergence of gradient em on multi-component mixture of gaussians. *Advances in Neural Information Processing Systems*, 30, 2017.
- Yurochkin, M., Agarwal, M., Ghosh, S., Greenewald, K., Hoang, N., and Khazaeni, Y. Bayesian nonparametric federated learning of neural networks. In *International Conference on Machine Learning*, pp. 7252–7261. PMLR, 2019.
- Zemel, R., Wu, Y., Swersky, K., Pitassi, T., and Dwork, C. Learning fair representations. In *International conference on machine learning*, pp. 325–333. PMLR, 2013.
- Zhang, J., Li, C., Robles-Kelly, A., and Kankanhalli, M. Hierarchically fair federated learning. 2020. URL <https://arxiv.org/pdf/2004.10386.pdf>.
- Zhang, X., Zhao, J., and LeCun, Y. Character-level convolutional networks for text classification. *Advances in neural information processing systems*, 28, 2015.
- Zhao, H. and Gordon, G. J. Inherent tradeoffs in learning fair representations. *Journal of Machine Learning Research*, 23(57):1–26, 2022. URL <http://jmlr.org/papers/v23/zhao21-1427.html>.
- Zhao, S., Sinha, A., He, Y., Perreault, A., Song, J., and Ermon, S. Comparing distributions by measuring differences that affect decision making. In *International Conference on Learning Representations*, 2022. URL <https://openreview.net/forum?id=KB5onONJIAU>.

A. Additional Experimental Results

A.1. Experimental Setups

Here we elaborate more details of our experiments.

Machines. We simulate the federated learning setup on a Linux machine with AMD Ryzen Threadripper 3990X 64-Core CPUs and 4 NVIDIA GeForce RTX 3090 GPUs.

Hyperparameters. For each FL experiment, we implement both FOCUS algorithm and FedAvg algorithm using SGD optimizer with the same hyperparameter setting. Detailed hyperparameter specifications are listed in Table 4 for different datasets, including learning rate, the number of local training steps, batch size, the number of training epochs, etc.

Table 4: Dataset description and hyperparameters.

Dataset	# training samples	# test samples	E	M	batch size	learning rate	local training epochs	epochs
MNIST	60000	10000	10	3	6000	0.1	10	300
CIFAR	50000	10000	10	2	100	0.1	2	300
Yelp/IMDB	56000/25000	38000/25000	10	2	512	5e-5	2	3

A.2. Comparison with existing fair FL methods

We present the full results of existing fair federated learning algorithms on our data settings in terms of FAA. The results in Tables 5 and 6 show that FOCUS achieves the lowest FAA score compared to existing fair FL methods. We note that fair FL methods (i.e., q-FFL (Li et al., 2020b) and AFL (Mohri et al., 2019)) have lower FAA scores than FedAvg, but their average test accuracy is worse. This is mainly because they mainly aim to improve bad agents (i.e., with high training loss), thus sacrificing the accuracy of agents with high-quality data.

Table 5: Comparison of FOCUS and the existing fair federated learning algorithms on the rotated MNIST dataset.

	FOCUS	FedAvg	q-FFL					AFL
			$q = 0.1$	$q = 1$	$q = 3$	$q = 5$	$q = 10$	$\lambda = 0.01$
Avg test accuracy	0.953	0.929	0.922	0.861	0.770	0.731	0.685	0.885
Avg test loss	0.152	0.246	0.269	0.489	0.777	0.900	1.084	0.429
FAA	0.094	0.363	0.388	0.612	0.547	0.419	0.253	0.220

Table 6: Comparison of FOCUS and the existing fair federated learning algorithms on the rotated CIFAR dataset.

	FOCUS	FedAvg	q-FFL					AFL
			$q = 0.1$	$q = 1$	$q = 3$	$q = 5$	$q = 10$	$\lambda = 0.01$
Avg test accuracy	0.688	0.654	0.648	0.592	0.426	0.181	0.121	0.661
Avg test loss	1.133	2.386	1.138	1.141	1.605	2.4746	2.526	1.666
FAA	0.360	1.115	0.620	0.473	0.384	0.313	0.379	0.595

A.3. Comparison with state-of-the-art FL methods

We compare FOCUS with other SOTA FL methods, including FedMA (Wang et al., 2020), Bayesian nonparametric FL (Yurochkin et al., 2019) and FedProx (Li et al., 2020a). Specifically, the matching algorithm in (Yurochkin et al., 2019) is designed for only fully-connected layers, and the matching algorithm in (Wang et al., 2020) is designed for fully-connected and convolutional layers, while our experiments on CIFAR use ResNet-18 where the batch norm layers and residual modules

are not considered in (Wang et al., 2020; Yurochkin et al., 2019). Therefore, we evaluate (Li et al., 2020a; Wang et al., 2020; Yurochkin et al., 2019) on MNIST with a fully-connected network, and (Li et al., 2020a) on CIFAR with a ResNet-18 model. The results on MNIST and CIFAR in Tables 7 and 8 show that FOCUS achieves the highest average test accuracy and lowest FAA score than SOTA FL methods.

Table 7: Comparison of FOCUS and other SOTA federated learning algorithms on the rotated MNIST dataset.

	FOCUS	FedAvg	FedProx			FedMA	Bayesian Nonparametric
			$\mu = 1$	$\mu = 0.1$	$\mu = 0.01$		
Avg test accuracy	0.953	0.929	0.908	0.927	0.929	0.753	0.517
Avg test loss	0.152	0.246	0.315	0.252	0.246	0.856	2.293
FAA	0.094	0.363	0.526	0.378	0.365	1.810	0.123

A.4. Scalability with more agents

To study the scalability of FOCUS, we evaluate the performance and fairness of FOCUS and existing methods under 100 clients on MNIST. Table 9 shows that FOCUS achieves the best fairness measured by FAA and Agnostic Loss, higher test accuracy, and lower test loss than Fedavg and existing fair FL methods.

A.5. Convergence of FOCUS

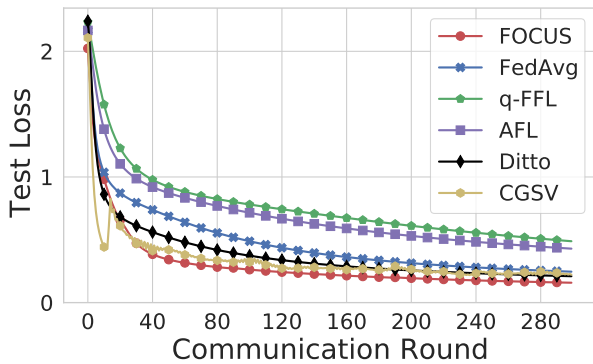
We report the test accuracy and test loss of different methods over FL communication rounds on Rotated MNIST with 10/100 clients and Rotated CIFAR in Figure 3. The results show that FOCUS converges faster and achieves higher accuracy and lower loss than other methods on both settings.

Table 8: Comparison of FOCUS and other SOTA federated learning algorithms on the rotated CIFAR dataset.

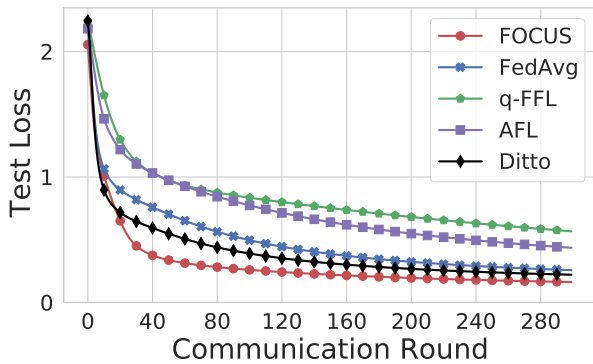
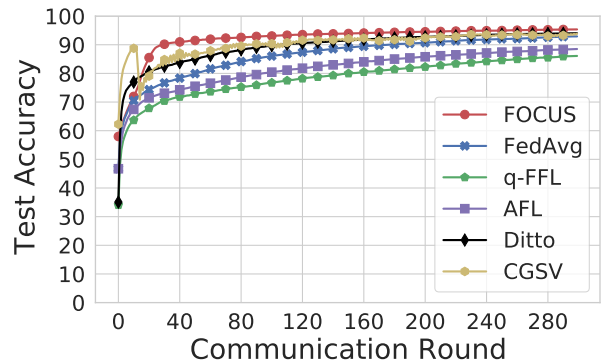
	FOCUS	FedAvg	FedProx		
			$\mu = 1$	$\mu = 0.1$	$\mu = 0.01$
Avg test accuracy	0.688	0.654	0.647	0.643	0.653
Avg test loss	1.133	2.386	1.206	2.151	2.404
FAA	0.360	1.115	0.397	0.884	0.787

Table 9: Comparison of different methods on MNIST 100 clients setting, in terms of average test accuracy (Avg Acc), average test loss (Avg Loss), fairness FAA and existing fairness metric Agnostic loss. FOCUS achieves the best fairness measured by FAA.

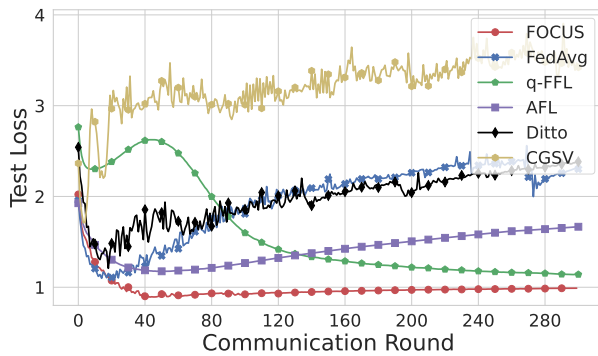
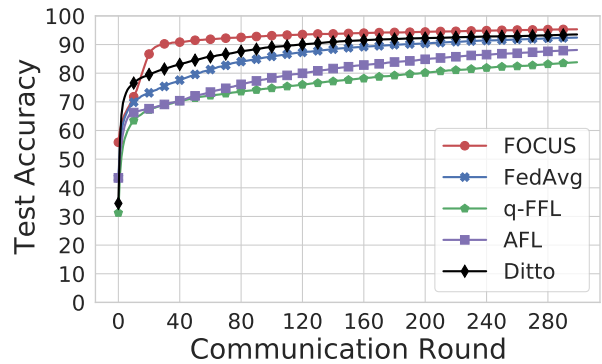
		FOCUS	FedAvg	q-FFL	AFL	Ditto	CGSV
				$q = 1$	$\lambda = 0.01$	$\lambda = 1$	$\beta = 1$
Rotated MNIST (100 clients)	Avg Acc	0.9533	0.9236	0.8371	0.8813	0.9351	0.8691
	Avg Loss	0.157	0.2571	0.5668	0.4355	0.2206	0.6294
	FAA	0.5605	1.0652	1.5055	0.8901	0.7459	1.2935
	Agnostic Loss	0.5028	0.8894	1.4227	0.7767	0.620	1.5133



(a) Rotated MNIST with 10 clients.



(b) Rotated MNIST with 100 clients.



(c) Rotated CIFAR with 10 clients.

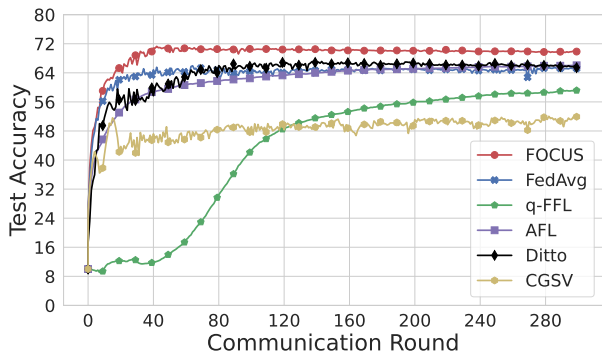


Figure 3: The test accuracy and test loss of different methods over FL communication rounds on different datasets. FOCUS converges faster and achieves higher accuracy and lower loss than other methods.

Table 10: Computation time of different FL fairness metric on Rotated MNIST. The computation of FAA is efficient under 10 clients and 100 client settings.

	10 clients	100 clients
Accuracy Parity (Li et al., 2020b)	4.70 e-05 second	6.48 e-05 second
Agnostic loss (Mohri et al., 2019)	9.41 e-07 second	3.92 e-06 second
FAA	6.09 e-06 second	4.27 e-05 second

Table 11: The number of communication rounds that different methods take to reach a target accuracy on Rotated MNIST. FOCUS requires a significantly smaller number of communication rounds than other methods.

	70%	80%	85%	90%
FOCUS	9	16	20	29
FedAvg	10	51	88	177
q-FFL	28	151	261	> 300
AFL	16	94	180	> 300

A.6. Runtime analysis

Computation time analysis for proposed metric FAA and its scalability to more clients. In FAA, to calculate the maximal difference of excess risks for any pair of agents, it suffices to calculate the difference between the maximal per-client excess risks and the minimum per-client excess risk, and we don’t need to calculate the difference for any pairs of agents. We compare the computation time (averaged over 100 trials) of FAA and existing fairness criteria (i.e., Accuracy Parity (Li et al., 2020b) and Agnostic Loss (Mohri et al., 2019)) under 10 clients and 100 clients on MNIST. Table 10 shows that the computation of FAA is efficient even with a large number of agents. Moreover, calculating the difference between maximal excess risk and minimum excess risk (i.e., FAA) is even faster than calculating the standard deviation of the accuracy between agents (i.e., Accuracy Parity).

Communication rounds analysis. Here, we report the number of communication rounds that each method takes to achieve targeted accuracy on MNIST and CIFAR in Table 11. We note that FOCUS requires significantly a smaller number of communication rounds than FedAvg, q-FFL, and AFL on both datasets, which demonstrates the small costs required by FOCUS.

Training time and inference time analysis. In terms of runtime, we report the training time for one FL round (averaged over 20 trials) as well as inference time (averaged over 100 trials) in Table 13. Since the local updates and sever aggregation for different cluster models can be run in parallel, we find that FOCUS has a similar training time compared to FedAvg, q-FFL, and AFL which train one global FL model. For the inference time, FOCUS is slightly slower than existing methods by about 0.17 seconds due to the ensemble prediction of all cluster models at each client. However, we note that such cost is

Table 12: The number of communication rounds that different methods take to reach a target accuracy on Rotated CIFAR. FOCUS requires a significantly smaller number of communication rounds than other methods.

	55%	60%	65%	70%
FOCUS	8	10	19	37
FedAvg	8	14	34	> 300
q-FFL	182	> 300	> 300	> 300
AFL	24	53	190	> 300

Table 13: Training time per FL round and inference time for different methods on Rotate MNIST.

	Training time per FL round	Inference time
FOCUS	6.59 second	0.28 second
FedAvg	6.23 second	0.12 second
q-FFL	6.32 second	0.11 second
AFL	6.24 second	0.12 second

Table 14: Comparison between FOCUS and FedAvg-HardCluster on Rotate MNIST under two scenarios.

	Scenario 1 (underly clusters are clearly separatable)		Scenario 2 (underly clusters are not separatable)	
	FOCUS	FedAvg-HardCluster	FOCUS	FedAvg-HardCluster
Avg test acc	0.953	0.954	0.814	0.812
Avg test loss	0.152	0.152	1.168	1.244
FAA	0.094	0.099	0.449	0.459
Agnostic loss	0.224	0.224	1.333	1.397

small and the forward passes of different cluster models for the ensemble prediction can also be made in parallel to further reduce the inference time.

A.7. Comparison to FedAvg with clustering

In this section, we construct a new method by combining the clustering and Fedavg together (i.e., FedAvg-HardCluster), which serves as a strong baseline. Specifically, FedAvg-HardCluster works as below:

- Step 1: before training, for each agent, it takes the arg max of the learned soft cluster assignment from FOCUS to get the hard cluster assignment (i.e., each agent only belongs to one cluster).
- Step 2: during training, each cluster then trains a FedAvg model based on corresponding agents.
- Step 3: during inference, each agent only uses the corresponding one cluster FedAvg model for inference.

To compare the performance between FOCUS and FedAvg-HardCluster, we consider two scenarios on MNIST:

- **Scenario 1:** underly clusters are clearly separatable, where each cluster contains samples from one distribution, which is the setting used in our paper.
- **Scenario 2:** underlying clusters are not separatable, where each cluster has 80%, 10%, and 10% samples from three different distributions, respectively. For example, the first underlying cluster contains 80% samples without rotation, 10% samples rotating 90 degrees, and 10% samples rotating 180 degrees.

We observe that the learned soft cluster assignments from FOCUS align with the underlying distribution, so the hard cluster assignment for Step 1 in FedAvg-HardCluster is equal to the underlying ground-truth clustering for both scenarios.

Table 14 presents the results of FOCUS and FedAvg-HardCluster on Rotated MNIST under two scenarios. **Under Scenario 1**, the accuracy of FOCUS and FedAvg-HardCluster is similar, and FOCUS achieves better fairness in terms of FAA. The results show that the hard clustering for FedAvg-HardCluster is as good as the soft clustering for FOCUS when the underlying clusters are clearly separatable, which verifies that clustering is one of the key steps in FOCUS, and it aligns with our hypothesis for fairness under heterogeneous data. **Under Scenario 2**, FOCUS achieves higher accuracy and better FAA fairness than FedAvg-HardCluster. The results show that when underly clusters are not separatable, soft clustering is better than hard clustering since each agent can benefit from multiple cluster models with the soft π learned from the EM algorithm in FOCUS.

Table 15: The effect of M on Rotate MNIST when the number of underlying clusters is 3.

	M=1	M=2	M=3	M=4
Avg test acc	0.929	0.952	0.953	0.953
Avg test loss	0.246	0.167	0.152	0.153
FAA	0.363	0.079	0.094	0.091
Agnostic loss	0.616	0.272	0.224	0.223

Table 16: The effect of M on Rotate CIFAR when the number of underlying clusters is 2.

	M=1	M=2	M=3	M=4
Avg test acc	0.654	0.688	0.696	0.693
Avg Loss	2.386	1.133	0.932	0.921
FAA	1.115	0.360	0.323	0.350
Agnostic loss	3.275	1.294	1.115	1.098

A.8. Effect of the number of the clusters M

The performance of FOCUS would not be harmed if the selected number of clusters is larger than the number of underlying clusters since the superfluous clusters would be useless (the corresponding soft cluster assignment π goes to zero). On the other hand, when the selected number of clusters is smaller than the number of underlying clusters, FOCUS would converge to a solution when some clusters contain agents from more than one underlying cluster.

Empirically, in Table 15, we have 3 true underlying clusters while we set $M = 1, 2, 3, 4$ in our experiments, and we see that when $M = 3$ and $M = 4$, FOCUS achieves similar accuracy and fairness, which verifies our hypothesis that the superfluous clusters would become useless. When $M = 2$, FOCUS even achieves the highest fairness, which might be because one cluster benefits from the shared knowledge of multiple underlying clusters. When $M = 1$, FOCUS reduces to FedAvg, which does not have the clustering mechanism, leading to the lowest accuracy and fairness under heterogeneous data.

A.9. Histogram of loss on CIFAR

Figure 4 shows the surrogate excess risk of every agent trained with FedAvg and FOCUS on CIFAR dataset. For the outlier cluster that rotates 180 degrees (i.e., 2nd cluster), FedAvg has the highest test loss for the 9th agent, resulting in a high excess risk of 2.74. In addition, the agents in 1st cluster trained by FedAvg are influenced by the FedAvg global model and have high excess risk. On the other hand, FOCUS successfully identifies the outlier distribution in 2nd cluster, leading to a much lower excess risk among agents with a more uniform excess risk distribution. Notably, FOCUS reduces the surrogate excess risk for the 9th agent to 0.44.

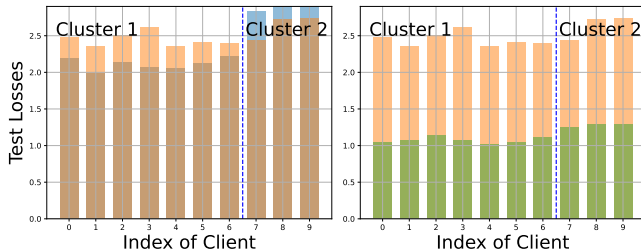


Figure 4: The excess risk of different agents trained with FedAvg (left) and FOCUS (right) on CIFAR dataset.

B. Convergence Proof

B.1. Convergence of Linear Models (Theorem 4.2)

B.1.1. KEY LEMMAS

We need to state two lemmas first before proving Theorem 4.2.

Lemma B.1. *Suppose $e \in S_m$ and the m -th cluster is the one closest to w_m^* . Assume $\|w_m^{(t)} - w_m^*\| \leq \alpha < \beta \leq \min_{m' \neq m} \|w_{m'}^{(t)} - w_m^*\|$. Then the E-step updates as*

$$\pi_{em}^{(t+1)} \geq \frac{\pi_{em}^{(t)}}{\pi_{em}^{(t)} + (1 - \pi_{em}^{(t)}) \exp\left(-(\beta^2 - \alpha^2 - 2(\alpha + \beta)r)\delta^2\right)} \quad (21)$$

Remark. Our assumption of proper initialization guarantees that $\|w_m^{(0)} - w_m^*\| \leq \alpha$ while $\forall m'$, we have $\|w_{m'} - w_m^*\|_2 \geq \|w_m^* - \mu_{m'}^*\| - \|w_{m'} - \mu_{m'}^*\| = R - \alpha$. Hence, we substitute $\beta = R - \alpha$ and $\alpha = \frac{R}{2} - r - \Delta$, which yields

$$\pi_{em}^{(t+1)} \geq \frac{\pi_{em}^{(t)}}{\pi_{em}^{(t)} + (1 - \pi_{em}^{(t)}) \exp(-2R\Delta\delta^2)}, \quad \forall e \in S_m \quad (22)$$

For M-steps, the local agents are initialized with $\theta_{em}^{(0)} = w_m^{(t)}$. Then for $k = 1, \dots, K - 1$, each agent use local SGD to update its personal model:

$$\theta_{em}^{(k+1)} = \theta_{em} - \eta_k g_{em}(\theta_{em}) = \theta_{em}^{(k)} - \eta_k \nabla \sum_{i=1}^{n_e} \ell(h_{\theta_{em}}(x_e^{(i)}), y_e^{(i)}). \quad (23)$$

To analyze the aggregated model Equation (6), we define a sequence of virtual aggregated models $\hat{w}_m^{(k)}$.

$$\hat{w}_m^{(k)} = \sum_{e=1}^E \frac{\pi_{em} \theta_{em}^{(k)}}{\sum_{e'=1}^E \pi_{e'm}}. \quad (24)$$

Lemma B.2. *Suppose any agent $e \in S_m$ has a soft clustering label $\pi_{em}^{(t+1)} \geq p$. Then one step of local SGD updates $\hat{w}_m^{(k)}$ by Equation (25), if the learning rate $\eta_k \leq \frac{1}{4\delta^2}$.*

$$\mathbb{E}\|\hat{w}_m^{(k+1)} - w_m^*\|_2^2 \leq (1 - 2\eta_k \gamma_m p \delta^2) \mathbb{E}\|\hat{w}_m^{(k)} - w_m^*\|_2^2 + \eta_k A_1 + \eta_k^2 A_2. \quad (25)$$

$$A_1 = 4\gamma_m r \delta^2 + 2\delta^2 E(1 - p), \quad A_2 = 16E(K - 1)^2 \delta^4 + O\left(\frac{d}{n_e}\right) E(\delta^4 + \delta^2 \sigma^2) \quad (26)$$

Remark. Using the recursive relation in Lemma B.2, if the learning rate η_k is fixed, the sequence $\hat{w}_m^{(k)}$ has a convergence rate of

$$\mathbb{E}\|\hat{w}_m^{(k)} - w_m^*\|_2^2 \leq (1 - 2\eta\gamma_m p \delta^2)^k \mathbb{E}\|\hat{w}_m^{(0)} - w_m^*\|_2^2 + \eta k (A_1 + \eta A_2). \quad (27)$$

B.1.2. COMPLETING THE PROOF OF THEOREM 4.2

We now combine Lemma B.1 and Lemma B.2 to prove Theorem 4.2. The theorem is restated below.

Theorem 4.2. *With the assumptions 1 and 2, $n_e = O(d)$, if learning rate $\eta \leq \min(\frac{1}{4\delta^2}, \frac{\beta}{\sqrt{T}})$,*

$$\pi_{em}^{(T)} \geq \frac{1}{1 + (M - 1) \cdot \exp(-2R\delta^2 \Delta_0 K)}, \quad \forall e \in S_m \quad (28)$$

$$\mathbb{E}\|w_m^{(T)} - w_m^*\|_2^2 \leq \left(1 - \frac{2\eta\gamma_m \delta^2}{M}\right)^{KT} (\|w_m^{(0)} - w_m^*\|_2^2 + A) + 2MKr + \frac{M\delta^2 E\beta}{2\sqrt{T}} O(K^3, \sigma^2). \quad (29)$$

where K is the total number of communication rounds; T is the number of iterations each round; $\gamma_m = |S_m|$ is the number of agents in the m -th cluster, and

$$A = \frac{2EK(M-1)\delta^2}{(1 - \frac{2\eta\delta^2\gamma_m}{M})^K - \exp(-2R\delta^2\Delta_0)}. \quad (30)$$

Proof. We prove Theorem 4.2 by induction. Suppose

$$\pi_{em}^{(t)} \geq \frac{1}{1 + (M-1)\exp(-2R\delta^2\Delta_0 t)} \quad (31)$$

$$\begin{aligned} \mathbb{E}\|w_m^{(t)} - w_m^*\|^2 &\leq (1 - \frac{2\eta\gamma_m\delta^2}{M})^{Kt} (\|w_m^{(0)} - w_m^*\|^2) + A \left((1 - \frac{2\eta\gamma_m\delta^2}{M})^{Kt} - \exp(-2R\delta^2\Delta_0 t) \right) \\ &\quad + \frac{\eta B}{1 - (1 - \frac{2\eta\gamma_m\delta^2}{M})^K}. \end{aligned} \quad (32)$$

where $B = [16E\delta^4 K^3 + EK(\delta^4 + \delta^2\sigma^2)]\eta + 4\gamma_m r\delta^2 K$.

Then according to Lemma B.1,

$$\pi_{em}^{(t+1)} \geq \frac{\pi_{em}^{(t)}}{\pi_{em}^{(t)} + (1 - \pi_{em}^{(t)})\exp(-2R\Delta_0\delta^2)} \quad (33)$$

$$\geq \frac{1}{1 + (M-1)\exp(-2R\delta^2\Delta_0 t)\exp(-2R\Delta_0\delta^2)} \quad (34)$$

$$\geq \frac{1}{1 + (M-1)\exp(-2R\Delta_0\delta^2(t+1))}. \quad (35)$$

We recall the virtual sequence of \hat{w}_m defined by Equation (24). Since models are synchronized after K rounds, the know $\hat{w}_m^{(0)} = w_m^{(t)}$ and $w_m^{(t+1)} = \hat{w}_m^{(K)}$. We then apply Lemma B.2 to prove the induction. Note that instead of proving Equation (29), we prove a stronger induction hypothesis of Equation (32).

$$\begin{aligned} \mathbb{E}\|w_m^{(t+1)} - w_m^*\|^2 &= \mathbb{E}\|\hat{w}_m^{(K)} - w_m^*\|^2 \end{aligned} \quad (36)$$

$$\leq (1 - 2\eta\gamma_m p\delta^2)^K \mathbb{E}\|\hat{w}_m^{(t)} - w_m^*\|^2 + \eta K(A_1 + \eta A_2) \quad (37)$$

$$\begin{aligned} &\leq (1 - 2\eta\gamma_m p\delta^2)^K \left((1 - \frac{2\eta\gamma_m\delta^2}{M})^{Kt} \|w_m^{(0)} - w_m^*\|^2 + A \left((1 - \frac{2\eta\gamma_m\delta^2}{M})^{Kt} - \exp(-2R\Delta_0\delta^2 t) \right) \right. \\ &\quad \left. + \frac{\eta B}{1 - (1 - \frac{2\eta\gamma_m\delta^2}{M})^K} \right) + \eta K(4\gamma_m r\delta^2 + 2\delta^2 E(1-p)) + \eta^2 K A_2 \end{aligned} \quad (38)$$

$$\begin{aligned} &\leq (1 - \frac{2\eta\gamma_m\delta^2}{M})^{(t+1)K} \|w_m^{(0)} - w_m^*\|^2 \\ &\quad + \underbrace{A(1 - \frac{2\eta\gamma_m\delta^2}{M})^{(t+1)K} - A \exp(-2R\Delta_0\delta^2 t)(1 - \frac{2\eta\gamma_m\delta^2}{M})^K + 2\delta^2 E(1-p)}_{D_1} \\ &\quad + \underbrace{(1 - \frac{2\eta\gamma_m\delta^2}{M})^K \frac{\eta B}{1 - (1 - \frac{2\eta\gamma_m\delta^2}{M})^K} + 4\eta K\gamma_m r\delta^2 + \eta^2 K A_2}_{D_2}. \end{aligned} \quad (39)$$

Note that $1 - p \leq (M-1)\exp(-2R\Delta_0\delta^2 t)$, so

$$\begin{aligned} D_1 &\leq A(1 - \frac{2\eta\gamma_m\delta^2}{M})^{(t+1)K} - A \exp(-2R\Delta_0\delta^2 t)(1 - \frac{2\eta\gamma_m\delta^2}{M})^K + 2\delta^2 EK(M-1)\exp(-2R\Delta_0\delta^2 t) \\ &\leq A \left((1 - \frac{2\eta\gamma_m\delta^2}{M})^{(t+1)K} - \exp(-2R\Delta_0\delta^2(t+1)) \right) \end{aligned} \quad (40)$$

For D_2 we have

$$\begin{aligned} D_2 &\leq \left(1 - \frac{2\eta\gamma_m\delta^2}{M}\right)^K \frac{\eta B}{\left[1 - \left(1 - \frac{2\eta\gamma_m\delta^2}{M}\right)^K\right]} + 4\eta\gamma_m r\delta^2 K + 16\eta^2 E\delta^4 K^3 + \eta^2 EKO(\delta^4 + \delta^2\sigma^2) \\ &= \frac{\eta B}{1 - \left(1 - \frac{2\eta\gamma_m\delta^2}{M}\right)^K}. \end{aligned} \quad (41)$$

Finally we combine Equations (39) to (41) so

$$\begin{aligned} \mathbb{E}\|w_m^{(t+1)} - w_m^*\|^2 &\leq \left(1 - \frac{2\eta\gamma_m\delta^2}{M}\right)^{(t+1)K} \|w_m^{(0)} - w_m^*\|^2 + A\left(\left(1 - \frac{2\eta\gamma_m\delta^2}{M}\right)^{(t+1)K} - \exp(-2R\delta^2\Delta_0(t+1))\right) \\ &\quad + \frac{\eta B}{1 - \left(1 - \frac{2\eta\gamma_m\delta^2}{M}\right)^K}. \end{aligned} \quad (42)$$

Since it is trivial to check that both induction hypotheses hold when $t = 0$, the induction hypothesis holds. Note that $K \geq 1$, so

$$\frac{\eta B}{1 - \left(1 - \frac{2\eta\gamma_m\delta^2}{M}\right)^K} \leq \eta B \frac{M}{2\eta\gamma_m\delta^2} \leq 2MKr + \frac{M\delta^2 E\beta}{2\sqrt{T}} O(K^3, \delta^2). \quad (43)$$

Combining Equation (42) and Equation (43) completes our proof. \square

B.1.3. DEFERRED PROOFS OF KEY LEMMAS

Lemma 1.

Proof. For simplicity, we abbreviate the model weights $w_m^{(t)}$ by w_m in the proof of this lemma. The n -th E step updates the weights Π by

$$\pi_{em}^{(t+1)} = \frac{\pi_{em}^{(t)} \exp[-\mathbb{E}_{(x,y)\sim D_e}(w_m^T x - y)^2]}{\sum_{m'} \pi_{em'}^{(t)} \exp[-\mathbb{E}_{(x,y)\sim D_e}(w_{m'}^T x - y)^2]} \quad (44)$$

so

$$\pi_{em}^{(t+1)} = \frac{\pi_{em}^{(t)} \exp(-\|w_m^{(t)} - \mu_e\|^2 \delta^2)}{\sum_{m'} \pi_{em'}^{(t)} \exp[-\|w_{m'}^{(t)} - \mu_e\|^2 \delta^2]} \quad (45)$$

$$\geq \frac{\pi_{em}^{(t)} \exp(-(\beta - r)^2 \delta^2)}{\pi_{em}^{(t)} \exp(-(\beta - r)^2 \delta^2) + \sum_{m' \neq m} \pi_{em'}^{(t)} \exp(-(\alpha + r)^2 \delta^2)} \quad (46)$$

$$\geq \frac{\pi_{em}^{(t)}}{\pi_{em}^{(t)} + (1 - \pi_{em}^{(t)}) \exp(-(\beta^2 - \alpha^2 - 2(\alpha + \beta)r)\delta^2)} \quad (47)$$

\square

Lemma 2.

Proof. Notice that local datasets are generated by $X_e \sim \mathcal{N}(0, \delta^2 \mathbf{1}^{n_e \times d})$ and $y_e = X_e \mu_e + \epsilon_e$ with $\epsilon_e \sim \mathcal{N}(0, \sigma^2)$. Therefore,

$$\|\hat{w}_m^{(k+1)} - w_m^*\|^2 = \|w_m^{(k)} - w_m^* - \eta_k g_k\|^2 \quad (48)$$

$$= \|\hat{w}_m^{(k)} - w_m^* - \eta_k \frac{2}{n_e} \sum_e \pi_{em} X_e^T X_e (\theta_{em}^{(k)} - \mu_e) + \frac{2\eta_k}{n_e} \sum_e \pi_{em} X_e^T \epsilon_e\|^2 \quad (49)$$

$$= \|\hat{w}_m^{(k)} - w_m^* - \hat{g}_k\|^2 + \eta_k^2 \|g_k - \hat{g}_k\|^2 + 2\eta_k \langle w_m^{(k)} - w_m^* - \hat{g}_k, \hat{g}_k - g_k \rangle. \quad (50)$$

where $\hat{g}_k = \frac{2}{n_e} \sum_e \pi_{em} \mathbb{E}(X_e^T X_e) (\theta_{em}^{(k)} - \mu)$. Since the expectation of the last term in Equation (50) is zero, we only need to estimate the expectation of $\|\hat{w}_m^{(k)} - w_m^* - \eta_k \hat{g}_k\|^2$ and $\|\hat{g}_k - g_k\|^2$.

$$\begin{aligned} & \|\hat{w}_m^{(k)} - w_m^* - \eta_k \hat{g}_k\|^2 \\ &= \|\hat{w}_m^{(k)} - w_m^*\|^2 + \frac{4\eta_k^2}{n_e^2} \sum_e \pi_{em} \mathbb{E}(X_e^T X_e) \|\theta_{em}^{(k)} - \mu_e\|^2 - \frac{4\eta_k}{n_e} \sum_e \pi_{em} \langle \hat{w}_m^{(k)} - w_m^*, \mathbb{E}(X_e^T X_e) (\theta_{em}^{(k)} - \mu_e) \rangle \\ &= \|\hat{w}_m^{(k)} - w_m^*\|^2 + 4\eta_k^2 \delta^2 \underbrace{\sum_e \pi_{em} \|\theta_{em}^{(k)} - \mu_e\|^2 - 4\eta_k \langle \hat{w}_m^{(k)} - w_m^*, \sum_e \pi_{em} \delta^2 (\theta_{em}^{(k)} - \mu_e) \rangle}_{C_1}. \end{aligned} \quad (51)$$

$$C_1 = -4\eta_k \sum_e \pi_{em} \langle \hat{w}_m^{(k)} - \theta_{em}^{(k)}, \delta^2 (\theta_{em}^{(k)} - \mu_e) \rangle - 4\eta_k \sum_e \pi_{em} \langle \theta_{em}^{(k)} - w_m^*, \delta^2 (\theta_{em}^{(k)} - \mu_e) \rangle \quad (52)$$

$$\begin{aligned} & \leq 4 \sum_e \pi_{em} \|\hat{w}_m^{(k)} - \theta_{em}^{(k)}\|^2 + 4\delta^4 \eta_k^2 \sum_e \pi_{em} \|\theta_{em}^{(k)} - \mu_e\|^2 - 4\eta_k \delta^2 \sum_e \pi_{em} \|\theta_{em}^{(k)} - \mu_e\|^2 \\ & \quad - 4\eta_k \delta^2 \underbrace{\sum_e \pi_{em} \langle \mu_e - w_m^*, \theta_{em}^{(k)} - \mu_e \rangle}_{C_2} \end{aligned} \quad (53)$$

Since $\eta_k \leq \frac{1}{4\delta^2}$,

$$\mathbb{E} \|\hat{w}_m^{(k)} - w_m^* - \eta_k \hat{g}_k\|^2 \quad (54)$$

$$\leq \mathbb{E} \|\hat{w}_m^{(k)} - w_m^*\|^2 + (8\delta^4 \eta_k^2 - 4\eta_k \delta^2) \sum_e \pi_{em} \mathbb{E} \|\theta_{em}^{(k)} - \mu_e\|^2 + 4 \sum_e \pi_{em} \mathbb{E} \|\hat{w}_m^{(k)} - \theta_{em}^{(k)}\|^2 + C_2 \quad (55)$$

$$\leq \mathbb{E} \|\hat{w}_m^{(k)} - w_m^*\|^2 - 2\eta_k \delta^2 \sum_e \pi_{em} \mathbb{E} \|\theta_{em}^{(k)} - \mu_e\|^2 + 4 \sum_e \pi_{em} \mathbb{E} \|\hat{w}_m^{(k)} - \theta_{em}^{(k)}\|^2 + C_2 \quad (56)$$

Note that

$$\sum_e \pi_{em} \mathbb{E} \|\theta_{em}^{(k)} - \mu_e\|^2 \quad (57)$$

$$= \sum_{e \in S_m} \pi_{em} \mathbb{E} \|\theta_{em}^{(k)} - \mu_e\|^2 + \sum_{e \notin S_m} \pi_{em} \mathbb{E} \|\theta_{em}^{(k)} - \mu_e\|^2 \quad (58)$$

$$\geq \sum_{e \in S_m} \pi_{em} (\mathbb{E} \|\theta_{em}^{(k)} - w_m^*\|^2 + 2r + r^2) + \sum_{e \notin S_m} \pi_{em} \mathbb{E} \|\theta_{em}^{(k)} - \mu_e\|^2 \quad (59)$$

$$= \sum_{e \in S_m} \pi_{em} (\mathbb{E} \|\hat{w}_m^{(k)} - w_m^*\|^2 + \mathbb{E} \|\hat{w}_m^{(k)} - \theta_{em}^{(k)}\|^2 + 2r + r^2) + \sum_{e \notin S_m} \pi_{em} \mathbb{E} \|\theta_{em}^{(k)} - \mu_e\|^2 \quad (60)$$

And since $\hat{w}_m^{(k)} = \mathbb{E} \sum_e \pi_{em} \theta_{em}^{(k)}$, we have

$$4\mathbb{E} \sum_e \pi_{em} \|\hat{w}_m^{(k)} - \theta_{em}^{(k)}\|^2 \leq 4\mathbb{E} \sum_e \pi_{em} \|\hat{w}_m^{(0)} - \theta_{em}^{(k)}\|^2 \quad (61)$$

$$\leq 4 \sum_e \pi_{em} (K-1) \mathbb{E} \sum_{t'}^{t-1} \eta_k'^2 \left\| \frac{2}{n_e} X_e^T X_e (\theta_{em}^{(k)} - \mu_e) \right\|^2 \quad (62)$$

$$\leq 16\eta_k^2 E (K-1)^2 \delta^4. \quad (63)$$

Thus,

$$\begin{aligned} \mathbb{E}\|\hat{w}_m^{(k)} - w_m^* - \eta_k \hat{g}_k\|^2 &\leq (1 - 2\eta_k \delta^2 \sum_e \pi_{em}) \mathbb{E}\|\hat{w}_m^{(k)} - w_m^*\|^2 + 16\eta_k^2 E(K-1)^2 \delta^4 \\ &\quad - \underbrace{2\eta_k \delta^2 \sum_{e \notin S_m} \pi_{em} \mathbb{E}\|\theta_{em}^{(k)} - \mu_e\|^2 - 4\eta_k \delta^2 \sum_e \pi_{em} \langle \theta_{em}^{(k)} - \mu_e, \mu_e - w_m^* \rangle}_{C_3} \end{aligned} \quad (64)$$

Since

$$C_3 \leq 2\eta_k \delta^2 \sum_{e \notin S_m} \pi_{em} \|\mu_e - w_m^*\|_2^2 - 4\eta_k \delta^2 \sum_{e \in S_m} \pi_{em} \|\theta_{em}^{(k)} - \mu_e\|_2 \|\mu_e - w_m^*\|_2 \quad (65)$$

$$\leq 2\eta_k \delta^2 E(1-p) + 4\eta_k \delta^2 \gamma_m r \quad (66)$$

we have

$$\mathbb{E}\|\hat{w}_m^{(k)} - w_m^* - \eta_k \hat{g}_k\|^2 \leq (2\eta_k \delta^2 \gamma_m p) \mathbb{E}\|\hat{w}_m^{(k)} - w_m^*\|^2 + 16\eta_k^2 E(K-1)^2 \delta^4 + 2\eta_k \delta^2 E(1-p) + 4\eta_k \delta^2 \gamma_m r \quad (67)$$

Notice that

$$\begin{aligned} \mathbb{E}\|\hat{g}_k - g_k\|^2 &= \mathbb{E} \sum_e \frac{4}{n_e^2} \pi_{em} \|(X_e^T X_e - \mathbb{E}(X_e^T X_e))(\theta_{em}^{(k)} - \mu_e)\|^2 + \mathbb{E} \sum_e \frac{4}{n_e^2} \sum_e \pi_{em} \|X_e^T \epsilon_e\|^2 \\ &= E \frac{O(dn_e)}{n_e^2} \delta^4 + E \frac{O(dn_e)}{n_e^2} \delta^2 \sigma^2 \end{aligned} \quad (68)$$

so

$$\mathbb{E}\|\hat{w}_m^{(k+1)} - w_m^*\|_2^2 \leq (1 - 2\eta_k \gamma_m p \delta^2) \mathbb{E}\|\hat{w}_m^{(k)} - w_m^*\|_2^2 + \eta_k A_1 + \eta_k^2 A_2 \quad (69)$$

where

$$A_1 = 4\delta^2 \gamma_m r + 2\delta^2 E(1-p) \quad (70)$$

and

$$A_2 = 16E(K-1)^2 \delta^4 + O\left(\frac{d}{n_e}\right) E(\delta^4 + \delta^2 \sigma^2). \quad (71)$$

□

B.2. Convergence of Models with Smooth and Strongly Convex Losses (Theorem 4.5)

Here we present the detailed proof for Theorem 4.5.

B.2.1. KEY LEMMAS

We first state two lemmas for E-step updates and M-step updates, respectively. The proofs of both lemmas are deferred to the Appendix B.2.3

Lemma B.3. *Suppose the loss function $\mathcal{L}_{P_t}(\theta)$ is L -smooth and μ -strongly convex for any cluster m . If $\|w_m^{(t)} - w_m^*\| \leq \frac{\sqrt{\mu R}}{\sqrt{\mu} + \sqrt{L}} - r - \Delta$ for some $\Delta > 0$, then E-step updates as*

$$\pi_{em}^{(t)} \geq \frac{\pi_{em}^{(t)}}{\pi_{em}^{(t)} + (1 - \pi_{em}^{(t)}) \exp(-\mu R \Delta)}. \quad (72)$$

For M-steps, the local agents are initialized with $\theta_{em}^{(0)} = w_m^{(t)}$. Then for $k = 1, \dots, K-1$, each agent use local SGD to update its personal model:

$$\theta_{em}^{(k+1)} = \theta_{em} - \eta_k g_{em}(\theta_{em}) = \theta_{em}^{(k)} - \eta_k \nabla \sum_{i=1}^{n_e} \ell(h_{\theta_{em}}(x_e^{(i)}), y_e^{(i)}). \quad (73)$$

To analyze the aggregated model Equation (6), we define a sequence of virtual aggregated models $\hat{w}_m^{(k)}$.

$$\hat{w}_m^{(k)} = \sum_{e=1}^E \frac{\pi_{em} \theta_{em}^{(k)}}{\sum_{e'=1}^E \pi_{e'm}}. \quad (74)$$

Lemma B.4. *Suppose for any agent $e \in S_m$, its soft clustering label $\pi_{em}^{(t+1)} \geq p$. Then one step local SGD updates $\hat{w}_m^{(k)}$ by Equation (75), if the learning rate $\eta_k \leq \frac{1}{2(\mu+L)}$.*

$$\mathbb{E} \|\hat{w}_m^{(k+1)} - w_m^*\|_2^2 \leq (1 - \eta_k A_0) \mathbb{E} \|\hat{w}_m^{(k)} - w_m^*\|_2^2 + \eta_k A_1 + \eta_k^2 A_2. \quad (75)$$

where

$$A_0 = \frac{2\gamma_m p \mu L}{\mu + L} \quad (76)$$

$$A_1 = 2\gamma_m L r \sqrt{\frac{2G}{\mu}} + \frac{G(1-p)E}{\mu} (4L + \frac{6}{\mu+L}) + O(r^2). \quad (77)$$

$$A_2 = \frac{4E(K-1)^2 G L^2}{\mu} + \frac{E\sigma^2}{n_e}. \quad (78)$$

Remark. Using this recursive relation, if the learning rate η_k is fixed, the sequence $\hat{w}_m^{(k+1)}$ has a convergence rate of

$$\mathbb{E} \|\hat{w}_m^{(k)} - w_m^*\|_2^2 \leq (1 - \eta A_0)^k \mathbb{E} \|\hat{w}_m^{(0)} - w_m^*\|_2^2 + \eta k (A_1 + \eta A_2). \quad (79)$$

B.2.2. COMPLETING THE PROOF OF THEOREM 4.5

Theorem 4.5. *Suppose loss functions have bounded variance for gradients on local datasets, i.e., $\mathbb{E}_{(x,y) \sim \mathcal{D}_e} [\|\nabla \ell(x, y; \theta) - \nabla \mathcal{L}_e(\theta)\|_2^2] \leq \sigma^2$. Assume population losses are bounded, i.e., $\mathcal{L}_e \in G, \forall e \in [E]$. With initialization from assumptions 3 and 4, if each agent chooses learning rate $\eta \leq \min(\frac{1}{2(\mu+L)}, \frac{\beta}{\sqrt{T}})$, the weights (Π, W) converges by*

$$\pi_{em}^{(T)} \geq \frac{1}{1 + (M-1) \exp(-\mu R \Delta_0 T)}, \quad \forall e \in S_m \quad (80)$$

$$\mathbb{E} \|w_m^{(T)} - w_m^*\|_2^2 \leq (1 - \eta A)^{KT} (\|w_m^{(0)} - w_m^*\|_2^2 + B) + O(Kr) + \frac{ME\beta O(K^3, \frac{\sigma^2}{n_e})}{\sqrt{T}} \quad (81)$$

where T is the total number of communication rounds; K is the number of iterations each round; $\gamma_m = |S_m|$ is the number of agents in the m -th cluster, and

$$A = \frac{2\gamma_m}{M} \frac{\mu L}{\mu + L}, B = \frac{GMTE(\frac{4L}{\mu} + \frac{6}{\mu(\mu+L)})}{(1 - \eta A)^K - \exp(-\mu R \Delta_0)}. \quad (82)$$

Proof. The proof is quite similar to Theorem 1 for linear models: we follow an induction proof using lemmas 3 and 4. Suppose Equation (80) hold for step t . And suppose

$$\mathbb{E} \|w_m^{(t)} - w_m^*\|_2^2 \leq (1 - \eta A)^{Kt} (\|w_m^{(0)} - w_m^*\|_2^2) + B((1 - \eta A)^{Kt} - \exp(-\mu R \Delta_0 t)) + \frac{\eta C}{1 - (1 - \eta A)^K}. \quad (83)$$

where

$$C = \frac{4\eta E G K^3 L^2}{\mu} + (2\gamma_m L r \sqrt{\frac{2G}{\mu}} + O(r^2)) + \eta \frac{EK\sigma^2}{n_e}. \quad (84)$$

Then for any $t \in S_m$,

$$\pi_{em}^{(t+1)} \geq \frac{\pi_{em}^{(t)}}{\pi_{em}^{(t)} + (1 - \pi_{em}^{(t)}) \exp(-\mu R \Delta_t)} \quad (85)$$

$$\geq \frac{1}{1 + (M-1) \exp(-\mu R \Delta_0 t) \exp(-\mu R \Delta_t)} \quad (86)$$

$$\geq \frac{1}{1 + (M-1) \exp(-\mu R \Delta_0 (t+1))} \quad (87)$$

We recall the virtual sequence $\hat{w}_m^{(k)}$ defined in Equation (74). Models are synchronized after K rounds of local iterations, so $w_m^{(t+1)} = \hat{w}_m^{(K)}$. Thus, according to Lemma B.4,

$$\mathbb{E}\|w_m^{(t+1)} - w_m^*\|_2^2 = \mathbb{E}\|\hat{w}_m^{(K)} - w_m^*\|_2^2 \quad (88)$$

$$\leq (1 - \eta A_0)^K \mathbb{E}\|w_m^{(t)} - w_m^*\|_2^2 + \eta K(A_1 + \eta A_2) \quad (89)$$

$$\leq (1 - \eta A_0)^K \left((1 - \eta A)^{Kt} (\mathbb{E}\|w_m^{(0)} - w_m^*\|_2^2) + B((1 - \eta A)^{Kt} - \exp(-\mu R \Delta_0 t)) + \frac{\eta C}{1 - (1 - \eta A)^K} \right) + \eta K(A_1 + \eta A_2) \quad (90)$$

$$\begin{aligned} &\leq (1 - \eta A)^{(t+1)K} \mathbb{E}\|w_m^{(0)} - w_m^*\|_2^2 + \underbrace{(1 - \eta A)^K B((1 - \eta A)^{Kt} - \exp(-\mu R \Delta_0 t)) + \eta \frac{GK(1-p)E}{\mu} (4L + \frac{6}{\mu+L})}_{F_1} \\ &\quad + \underbrace{(1 - \eta A)^K \frac{\eta C}{1 - (1 - \eta A)^K} + \eta K(2\gamma_m L r \sqrt{\frac{2G}{\mu}} + O(r^2)) + \eta^2 K A_2}_{F_2}. \end{aligned} \quad (91)$$

For F_1 , we use the fact that

$$\pi_{em}^{(t+1)} \geq \frac{1}{1 + (M-1) \exp(-\mu R \Delta_0 (t+1))} \geq 1 - (M-1) \exp(-\mu R \Delta_0 (t+1)),$$

so

$$F_1 \leq (1 - \eta A)^K B((1 - \eta A)^{Kt} - \exp(-\mu R \Delta_0 t)) + \eta \frac{G(M-1) \exp(-\mu R \Delta_0 t)}{\mu} (4L + \frac{6}{\mu+L}) \quad (92)$$

$$= B((1 - \eta A)^{(t+1)K} - \exp(-\mu R \Delta_0 t)) \quad (93)$$

For F_2 , we have

$$F_2 \leq (1 - \eta A)^K \frac{\eta C}{1 - (1 - \eta A)^K} + \eta K(2\gamma_m L r \sqrt{\frac{2G}{\mu}} + O(r^2)) + \frac{4EGL^2 \eta^2 K^3}{\mu} + \frac{\eta^2 K E \sigma^2}{n_e} \quad (94)$$

$$\leq \frac{\eta C}{1 - (1 - \eta A)^K}. \quad (95)$$

Combining F_1 and F_2 finishes the induction proof. Moreover, since $T \geq 1$, we have

$$\frac{\eta C}{1 - (1 - \eta A)^K} \leq \frac{C}{A} = O(Kr) + \frac{ME\beta}{\sqrt{T}} O(K^3, \frac{\sigma^2}{n_e}). \quad (96)$$

Combining Equation (83) and Equation (96) completes our proof. \square

B.2.3. DEFERRED PROOFS OF KEY LEMMAS

Lemma 3.

Proof. According to Algorithm 1,

$$\pi_{em}^{(t+1)} = \frac{\pi_{em}^{(t)}}{\pi_{em}^{(t)} + \sum_{m' \neq m} \pi_{em'}^{(t)} \exp\left(\mathbb{E}\ell(x, y; w_m^{(t)}) - \mathbb{E}\ell(x, y; w_{m'}^{(t)})\right)} \quad (97)$$

$$\geq \frac{\pi_{em}^{(t)}}{\pi_{em}^{(t)} + (1 - \pi_{em}^{(t)}) \exp\left(\max_{m' \neq m} (\mathcal{L}_{P_e}(w_m^{(t)}) - \mathcal{L}_{P_e}(w_{m'}^{(t)}))\right)} \quad (98)$$

Since \mathcal{L}_{P_e} is L -smooth and μ -strongly convex,

$$\begin{aligned} \mathcal{L}_{P_e}(w_m^{(t)}) - \mathcal{L}_{P_e}(w_m^{(t')}) &\leq \frac{L}{2} \|w_m^{(t)} - \theta_t^*\|^2 - \frac{\mu}{2} \|w_m^{(t)} - \theta_t^*\|^2 \\ &\leq \frac{L}{2} \left(\frac{\sqrt{\mu}R}{\sqrt{\mu} + \sqrt{L}} - \Delta \right)^2 - \frac{\mu}{2} \left(\frac{\sqrt{L}R}{\sqrt{\mu} + \sqrt{L}} + \Delta \right)^2 \\ &\leq -\sqrt{\mu LR}\Delta + \frac{L - \mu}{2} \Delta^2 \leq -\mu R\Delta. \end{aligned} \quad (99)$$

Combining Equation (98) and Equation (99) completes our proof. \square

Lemma 4.

Proof. We define $g_m^{(k)} = \sum_e \pi_{em} \frac{1}{n_e} \sum_{i=1}^{n_e} \nabla \ell(h_{\theta_{em}}(x_e^{(i)}), y_e^{(i)})$ and $\hat{g}_m^{(k)} = \sum_e \pi_{em} \nabla \mathcal{L}(\theta_{em}^{(k)})$.

$$\mathbb{E} \|\hat{w}_m^{(k+1)} - w_m^*\|^2 = \mathbb{E} \|\hat{w}_m^{(k)} - w_m^* - \eta_k g_m^{(k)}\|^2 \quad (100)$$

$$\begin{aligned} &= \mathbb{E} \|\hat{w}_m^{(k)} - w_m^* - \eta_k \hat{g}_m^{(k)}\|^2 + \eta_k^2 \mathbb{E} \|g_m^{(k)} - \hat{g}_m^{(k)}\|^2 \\ &\quad + 2\eta_k \mathbb{E} \langle w_m^{(k)} - w_m^* - \eta_k \hat{g}_m^{(k)}, \hat{g}_m^{(k)} - g_m^{(k)} \rangle \end{aligned} \quad (101)$$

$$= \mathbb{E} \|\hat{w}_m^{(k)} - w_m^* - \eta_k \hat{g}_m^{(k)}\|^2 + \eta_k^2 \mathbb{E} \|g_m^{(k)} - \hat{g}_m^{(k)}\|^2. \quad (102)$$

The first term can be decomposed into

$$\|\hat{w}_m^{(k)} - w_m^* - \eta_k \hat{g}_m^{(k)}\|^2 = \|\hat{w}_m^{(k)} - w_m^*\|^2 + \eta_k^2 \|\hat{g}_m^{(k)}\|^2 - 2\eta_k \langle \hat{w}_m^{(k)} - w_m^*, \hat{g}_m^{(k)} \rangle. \quad (103)$$

Note that

$$\|\hat{g}_m^{(k)}\|^2 \leq \sum_{e=1}^E \pi_{em} \|\nabla \mathcal{L}_e(\theta_{em}^{(k)})\|^2. \quad (104)$$

$$- \langle \hat{w}_m^{(k)} - w_m^*, \hat{g}_m^{(k)} \rangle = - \sum_{e=1}^E \pi_{em} \langle \hat{w}_m^{(k)} - \theta_{em}^{(k)}, \nabla \mathcal{L}_e(\theta_{em}^{(k)}) \rangle - \sum_{e=1}^E \pi_{em} \langle \theta_{em}^{(k)} - w_m^*, \nabla \mathcal{L}_e(\theta_{em}^{(k)}) \rangle. \quad (105)$$

We further decompose the two terms in Equation (105) by

$$-2 \langle \hat{w}_m^{(k)} - \theta_{em}^{(k)}, \nabla \mathcal{L}_e(\theta_{em}^{(k)}) \rangle \leq \frac{1}{\eta_k} \|\hat{w}_m^{(k)} - \theta_{em}^{(k)}\|^2 + \eta_k \|\nabla \mathcal{L}_e(\theta_{em}^{(k)})\|^2. \quad (106)$$

and

$$\langle \theta_{em}^{(k)} - w_m^*, \nabla \mathcal{L}_e(\theta_{em}^{(k)}) \rangle \geq \langle \theta_{em}^{(k)} - w_m^*, \nabla \mathcal{L}_e(\theta_{em}^{(k)}) - \nabla \mathcal{L}_e(w_m^*) \rangle - \|\nabla \mathcal{L}_e(w_m^*)\|_2 \|\theta_{em}^{(k)} - w_m^*\|_2. \quad (107)$$

$$\geq \frac{\mu L}{\mu + L} \|\theta_{em}^{(k)} - w_m^*\|^2 + \frac{1}{\mu + L} \|\nabla \mathcal{L}_e(\theta_{em}^{(k)}) - \nabla \mathcal{L}_e(w_m^*)\|^2 - \|\nabla \mathcal{L}_e(w_m^*)\|_2 \|\theta_{em}^{(k)} - w_m^*\|_2. \quad (108)$$

Therefore,

$$\begin{aligned} \mathbb{E} \|\hat{w}_m^{(k+1)} - w_m^*\|^2 &\leq \underbrace{\mathbb{E} \|\hat{w}_m^{(k)} - w_m^*\|^2}_{E_1} - 2\eta_k \underbrace{\frac{\mu L}{\mu + L} \sum_e \pi_{em} \mathbb{E} \|\theta_{em}^{(k)} - w_m^*\|^2}_{E_2} + \underbrace{\sum_e \pi_{em} \mathbb{E} \|\hat{w}_m^{(k)} - \theta_{em}^{(k)}\|^2}_{E_2} \\ &\quad + \underbrace{\left(2\eta_k^2 \sum_e \pi_{em} \mathbb{E} \|\nabla \mathcal{L}_e(\theta_{em}^{(k)})\|^2 - 2\eta_k \frac{1}{\mu + L} \sum_e \pi_{em} \mathbb{E} \|\nabla \mathcal{L}_e(\theta_{em}^{(k)}) - \nabla \mathcal{L}_e(w_m^*)\|^2 \right)}_{E_3} \\ &\quad + \underbrace{2\eta_k \mathbb{E} \sum_e \pi_{em} \|\theta_{em}^{(k)} - w_m^*\|_2 \cdot \|\nabla \mathcal{L}_e(w_m^*)\|_2}_{E_4} + \underbrace{\eta_k^2 \mathbb{E} \|g_m^{(k)} - \hat{g}_m^{(k)}\|^2}_{E_5}. \end{aligned} \quad (109)$$

□

$$\begin{aligned}
 E_1 &= \mathbb{E} \|\hat{w}_m^{(k)} - w_m^*\|^2 - 2\eta_k \frac{\mu L}{\mu + L} \mathbb{E} \left(\sum_e \pi_{em} \|\hat{w}_m^{(k)} - w_m^*\|^2 + \sum_e \pi_{em} \|\hat{w}_m^{(k)} - \theta_{em}^{(k)}\|^2 \right) \\
 &\leq \left(1 - \frac{2\eta_k \mu L p \gamma_m}{\mu + L}\right) \mathbb{E} \|w_m^{(k)} - w_m^*\|^2 + E_2.
 \end{aligned} \tag{110}$$

$$\begin{aligned}
 E_2 &= \mathbb{E} \sum_e \pi_{em} \|\hat{w}_m^{(k)} - \theta_{em}^{(k)}\|^2 \\
 &= \mathbb{E} \sum_e \pi_{em} \|(w_m^{(0)} - \theta_{em}^{(k)}) + (\theta_{em}^{(k)} - w_m^{(k)})\|^2 \\
 &\leq \mathbb{E} \sum_e \pi_{em} \|(w_m^{(0)} - \theta_{em}^{(k)})\|^2 \\
 &\leq \sum_e \pi_{em} (K-1) \mathbb{E} \sum_{k'=0}^{k-1} \eta_{k'}^2 \|g_{em}(\theta_{em}^{(k')})\|^2 \\
 &\leq \frac{2\eta_k^2 E (K-1)^2 G^2 L^2}{\mu}.
 \end{aligned} \tag{111}$$

$$\begin{aligned}
 E_3 &= 2\mathbb{E} \sum_e \pi_{em} \left(\left(\eta_k^2 - \frac{\eta_k}{\mu + L} \right) \|\nabla \mathcal{L}_e(\theta_{em}^{(k)})\|^2 + \frac{2\eta_k}{\mu + L} \langle \nabla \mathcal{L}_e(\theta_{em}^{(k)}), \nabla \mathcal{L}_e(w_m^*) \rangle - \eta_k \frac{\|\nabla \mathcal{L}_e(w_m^*)\|^2}{\mu + L} \right) \\
 &\leq 4\eta_k \mathbb{E} \sum_e \pi_{em} \left(-\frac{1}{2(\mu + L)} \|\nabla \mathcal{L}_e(\theta_{em}^{(k)})\|^2 + \frac{1}{\mu + L} \langle \nabla \mathcal{L}_e(\theta_{em}^{(k)}), \nabla \mathcal{L}_e(w_m^*) \rangle - \frac{\|\nabla \mathcal{L}_e(w_m^*)\|^2}{\mu + L} \right) \\
 &\leq 6\eta_k \sum_e \pi_{em} \frac{\|\nabla \mathcal{L}_e(w_m^*)\|^2}{\mu + L} \\
 &\leq 6\eta_k \sum_{e \in S_m} \pi_{em} \frac{L^2 r^2}{\mu + L} + 6\eta_k \sum_{e \notin S_m} \pi_{em} \frac{2G}{\mu(\mu + L)} \\
 &\leq \eta_k O(r^2) + 6\eta_k \frac{G(1-p)E}{\mu(\mu + L)}.
 \end{aligned} \tag{112}$$

$$\begin{aligned}
 E_4 &= 2\eta_k \mathbb{E} \sum_{e \in S_m} \pi_{em} \|\theta_{em}^{(k)} - w_m^*\|_2 \cdot \|\nabla \mathcal{L}_e(w_m^*)\|_2 + 2\eta_k \mathbb{E} \sum_{e \notin S_m} \pi_{em} \|\theta_{em}^{(k)} - w_m^*\|_2 \cdot \|\nabla \mathcal{L}_e(w_m^*)\|_2 \\
 &\leq 2\eta_k \gamma_m L r \sqrt{\frac{2G}{\mu}} + 2\eta_k (1-p) E L \cdot \frac{2G}{\mu}.
 \end{aligned} \tag{113}$$

$$\begin{aligned}
 E_5 &= \eta_k^2 \mathbb{E} \|g_m^{(k)} - \hat{g}_m^{(k)}\|^2 \\
 &\leq \eta_k^2 \mathbb{E} \left\| \sum_e \pi_{em} \left(\frac{1}{n_e} \sum_{i=1}^{n_e} \nabla \ell(h_{\theta_{em}}(x_e^{(i)}), y_e^{(i)}) - \mathcal{L}(\theta_{em}^{(k)}) \right) \right\|^2 \\
 &\leq \eta_k^2 E \frac{\sigma^2}{n_e}.
 \end{aligned} \tag{114}$$

Combining Equation (110) to Equation (114) yields the conclusion of Lemma B.4.

C. Fairness Analysis

C.1. Proof of Theorem 4.6

Proof. Let the first cluster m_1 contain agents μ_1, \dots, μ_{E-1} , while the second cluster contains only the outlier μ_E . Then, for $e = 1, \dots, E-1$,

$$\mathcal{E}_e(w_{m_1}) = \delta^2 \left\| \mu_e - \frac{\sum_{e'=1}^{E-1} \mu_{e'}}{E-1} \right\|^2 \leq \delta^2 r^2 \quad (115)$$

And for the outlier agent, the expected output is just the optimal solution, so

$$\mathcal{E}_E(w_{m_2}) = 0 \quad (116)$$

As a result, the fairness of this algorithm is bounded by

$$\mathcal{FAA}_{focus}(P) = \max_{i,j \in [E]} |\mathcal{E}_i(\Pi, W) - \mathcal{E}_j(\Pi, W)| \leq \delta^2 r^2. \quad (117)$$

On the other hand, the expected final weights of FedAvg algorithm is $w_{avg} = \bar{\mu} = \frac{\sum_{e=1}^E \mu_e}{E}$, so the expected loss for agent e shall be

$$\mathbb{E}_{(x,y) \sim \mathcal{P}_e}(\ell_{\hat{\theta}}(x)) = \mathbb{E}_{x \sim \mathcal{N}(0, \delta^2 I_d), \epsilon \sim \mathcal{N}(0, \sigma_e^2)}[(\mu_i^T x + \epsilon - \bar{\mu}^T x)^2] = \sigma_e^2 + \delta^2 \|\mu_e - \bar{\mu}\|^2 \quad (118)$$

The infimum risk for agent t_1 is σ_1^2 , and after subtracting it from the expected loss, we have

$$\mathcal{E}_1(w_{avg}) = \delta^2 \|\mu_1 - \bar{\mu}\|^2 \quad (119)$$

$$= \delta^2 \left\| \mu_1 - \frac{\sum_{e=1}^{E-1} \mu_1}{E} - \frac{\mu_E}{E} \right\|^2 \quad (120)$$

$$\leq \delta^2 \left(r \cdot \frac{E-1}{E} + \frac{\|\mu_1 - \mu_E\|}{E} \right)^2 \quad (121)$$

$$\leq \delta^2 \left(r \cdot \frac{E-1}{E} + \frac{R+r}{E} \right)^2 = \delta^2 \left(r + \frac{R}{E} \right)^2 \quad (122)$$

However for the outlier agent,

$$\mathcal{E}_E(w_{avg}) = \delta^2 \|\mu_E - \bar{\mu}\|^2 \quad (123)$$

$$= \delta^2 \left\| \frac{E-1}{E} \mu_E - \frac{\sum_{e=1}^{E-1} \mu_E}{E} \right\|^2 \quad (124)$$

$$\geq \left(\frac{E-1}{E} \right)^2 \delta^2 R^2 \quad (125)$$

Hence,

$$\mathcal{FAA}_{avg}(P) \geq \mathcal{E}_E(w_{avg}) - \mathcal{E}_1(w_{avg}) = \delta^2 \left(\frac{R^2(E-2) - 2Rr}{E} + r^2 \right) \quad (126)$$

□

Remark. When there are $E_k > 1$ outliers, we can similarly derive FAA for FedAvg algorithm:

$$\mathcal{E}_1(w_{avg}) \leq \delta^2 \left(r + \frac{E_k R}{E} \right)^2 \quad (127)$$

$$\mathcal{E}_E(w_{avg}) \geq \delta^2 \left(\frac{E - E_k}{E} R - \frac{E_k}{E} r \right)^2 \quad (128)$$

so as long as $E_k < \frac{E}{2}$,

$$\mathcal{FAA}_{avg} \geq \mathcal{E}_E(w_{avg}) - \mathcal{E}_1(w_{avg}) = \Omega(\delta^2 R^2) \quad (129)$$

The FOCUS algorithm produces a result with

$$\mathcal{E}_1(w_{m_1}) \leq \delta^2 r^2 \quad (130)$$

$$\mathcal{E}_E(w_{m_2}) \leq \delta^2 r^2 \quad (131)$$

Hence we still have

$$\mathcal{FAA}_{focus} \leq \delta^2 r^2. \quad (132)$$

C.2. Proof of Theorem 4.7

Proof. Note that the local population loss for agent i with weights θ is

$$\mathcal{L}_i(\theta) = \int p_i(x, y) \ell(f_\theta(x), y) dx dy. \quad (133)$$

Thus,

$$|\mathcal{L}_i(\theta_i^*) - \mathcal{L}_j(\theta_j^*)| = \int |p_i(x, y) - p_j(x, y)| \cdot \ell(f_{\theta_i^*}(x), y) dx dy \quad (134)$$

$$\leq G \cdot \int |p_i(x, y) - p_j(x, y)| dx dy \leq Gr. \quad (135)$$

Hence,

$$\mathcal{L}_i(\theta_j^*) \leq \mathcal{L}_j(\theta_j^*) + Gr \leq \mathcal{L}_j(\theta_i^*) + Gr \leq \mathcal{L}_i(\theta_i^*) + 2Gr. \quad (136)$$

For the cluster that combines agents $\{1, \dots, E-1\}$ together, the weight converges to $\bar{\theta}' = \frac{1}{E-1} \sum_{i=1}^{E-1} \theta_i^*$. Then $\forall i = 1, \dots, E-1$, the population loss for the ensemble prediction

$$\mathcal{L}_i(\theta, \Pi) = \mathcal{L}_i\left(\frac{\sum_{j=1}^{E-1} \theta_j^*}{E-1}\right) \quad (137)$$

$$\leq \frac{1}{T-1} \sum_{j=1}^{T-1} \mathcal{L}_i(\theta_j^*) \quad (138)$$

$$\leq \mathcal{L}_i(\theta_i^*) + \frac{2Gr}{E-1}. \quad (139)$$

Therefore, for any $i = 1, \dots, T-1$,

$$\mathcal{E}_i(\theta, \Pi) \leq \frac{2Gr}{E-1}. \quad (140)$$

Since $\mathcal{E}_T(\theta, \Pi) = 0$,

$$\mathcal{FAA}_{focus}(W, \Pi) \leq \frac{2Gr}{E-1} \quad (141)$$

Now we prove the second part of Theorem 4.7 for the fairness of Fedavg algorithm. For simplicity, we define $B = \frac{2Gr}{E-1}$ in this proof. Also, we denote the mean of all optimal weight $\bar{\theta} = \frac{\sum_{i=1}^E \theta_i^*}{E}$ and $\bar{\theta}' = \frac{\sum_{i=1}^{E-1} \theta_i^*}{E-1}$.

Remember that we assume loss functions to be L -smooth, so

$$\mathcal{L}_E(\theta_i^*) \leq \mathcal{L}_E(\bar{\theta}') + \langle \nabla \mathcal{L}_E(\bar{\theta}'), \theta_i^* - \bar{\theta}' \rangle + \frac{L}{2} \|\bar{\theta}' - \theta_i^*\|^2. \quad (142)$$

Taking summation over $i = 1, \dots, E-1$, we get

$$\mathcal{L}_E(\bar{\theta}') \geq \frac{1}{E-1} \left(\sum_{i=1}^{E-1} \mathcal{L}_E(\theta_i^*) - \langle \nabla \mathcal{L}_E(\bar{\theta}'), \sum_{i=1}^{E-1} (\theta_i^* - \bar{\theta}') \rangle - \frac{L}{2} \sum_{i=1}^{E-1} \|\bar{\theta}' - \theta_i^*\|^2 \right) \quad (143)$$

$$= \frac{1}{E-1} \left(\sum_{i=1}^{E-1} \mathcal{L}_E(\theta_i^*) - \frac{L}{2} \sum_{i=1}^{E-1} \|\bar{\theta}' - \theta_i^*\|^2 \right) \quad (144)$$

$$\geq \mathcal{L}_E(\theta_E^*) + R - \frac{LB}{\mu}. \quad (145)$$

The last inequality uses the μ -strongly convex condition that implies

$$B \geq \mathcal{L}_i(\bar{\theta}') - \mathcal{L}_i(\theta_i^*) \geq \frac{\mu}{2} \|\bar{\theta}' - \theta_i^*\|^2. \quad (146)$$

By L -smoothness, we have

$$\mathcal{L}_E(\bar{\theta}') \leq \mathcal{L}_E(\bar{\theta}) + \langle \nabla \mathcal{L}_E(\bar{\theta}), \bar{\theta}' - \bar{\theta} \rangle + \frac{L}{2} \|\bar{\theta}' - \bar{\theta}\|^2. \quad (147)$$

$$\mathcal{L}_E(\theta_E^*) \leq \mathcal{L}_E(\bar{\theta}) + \langle \nabla \mathcal{L}_E(\bar{\theta}), \theta_E^* - \bar{\theta} \rangle + \frac{L}{2} \|\theta_E^* - \bar{\theta}\|^2. \quad (148)$$

Note that $\bar{\theta} = \frac{\bar{\theta}' + (E-1)\theta_E^*}{E}$, we take a weighted sum over the above two inequalities to cancel the dot product terms out. We thus derive

$$\mathcal{L}_E(\bar{\theta}) \geq \frac{(E-1)\mathcal{L}_E(\bar{\theta}') + \mathcal{L}_E(\theta_E^*) - \frac{L}{2}(E-1)\|\bar{\theta}' - \bar{\theta}\|^2 - \frac{L}{2}\|\theta_E^* - \bar{\theta}\|^2}{E} \quad (149)$$

$$= \frac{E-1}{E} \left(R - \frac{LB}{\mu} - \frac{L\|\theta_E^* - \bar{\theta}'\|^2}{2E} \right) + \mathcal{L}_E(\theta_E^*). \quad (150)$$

Note that $\mathcal{L}_E(\cdot)$ is μ -strongly convex, which means

$$R - \frac{LB}{\mu} \geq \mathcal{L}_E(\bar{\theta}') - \mathcal{L}_E(\theta_E^*) \geq \frac{\mu}{2} \|\theta_E^* - \bar{\theta}'\|^2. \quad (151)$$

so

$$\mathcal{L}_E(\bar{\theta}) \geq \left(1 - \frac{L}{\mu E}\right) \cdot \frac{E-1}{E} \left(R - \frac{LB}{\mu}\right) + \mathcal{L}_E(\theta_E^*). \quad (152)$$

And

$$\mathcal{E}_E(\bar{\theta}) \geq \left(1 - \frac{L}{\mu E}\right) \cdot \frac{E-1}{E} \left(R - \frac{LB}{\mu}\right). \quad (153)$$

On the other hand, for agent $i = 1, \dots, E-1$ we know

$$\mathcal{L}_i(\bar{\theta}) \leq \mathcal{L}_i(\bar{\theta}') + \langle \nabla \mathcal{L}_i(\bar{\theta}'), \bar{\theta} - \bar{\theta}' \rangle + \frac{L}{2} \|\bar{\theta} - \bar{\theta}'\|^2. \quad (154)$$

By L smoothness,

$$\|\nabla \mathcal{L}_i(\bar{\theta}')\|_2 \leq L \|\bar{\theta}' - \theta_i^*\| \leq L \sqrt{\frac{2B}{\mu}}. \quad (155)$$

So

$$\mathcal{L}_i(\bar{\theta}) \leq \mathcal{L}_i(\theta_i^*) + B + L \sqrt{\frac{2B}{\mu}} \sqrt{\frac{2(R - \frac{LB}{\mu})}{\mu}} \frac{1}{E} + \frac{L(R - \frac{LB}{\mu})}{\mu E^2} \quad (156)$$

$$\mathcal{E}_i(\bar{\theta}) \leq B + \frac{2L}{\mu E} \sqrt{B(R - \frac{LB}{\mu})} + \frac{L(R - \frac{LB}{\mu})}{\mu E^2} \quad (157)$$

In conclusion, the fairness can be estimated by

$$\mathcal{FAA}_{avg}(P) \geq \mathcal{E}_E(\bar{\theta}) - \mathcal{E}_1(\bar{\theta}) \quad (158)$$

$$\geq \left(\frac{E-1}{E} - \frac{L}{\mu E^2}\right) R - \left(1 + \frac{L(E-1)}{\mu E} - \frac{L^2}{\mu^2 E}\right) B - \frac{2L}{\mu E} \sqrt{B(R - \frac{L}{\mu} B)} \quad (159)$$

□

C.3. Proof of Divergence Reduction

Here we prove the claim that the assumption $\mathcal{L}_E(\theta_e^*) - \mathcal{L}_E(\theta_E^*) \geq R$ is implied by a lower bound of the H-divergence (Zhao et al., 2022).

$$D_H(\mathcal{P}_e, \mathcal{P}_E) \geq \frac{LR}{4\mu} \quad (160)$$

Proof. Note that

$$D_H(\mathcal{P}_e, \mathcal{P}_E) = \frac{1}{2} \min_{\theta} \left(\mathcal{L}_e(\theta) + \mathcal{L}_E(\theta) \right) + \frac{1}{2} \left(\mathcal{L}_e(\theta_e^*) + \mathcal{L}_E(\theta_E^*) \right) \quad (161)$$

$$\leq \frac{1}{2} \left(\mathcal{L}_e\left(\frac{\theta_e^* + \theta_E^*}{2}\right) + \mathcal{L}_E\left(\frac{\theta_e^* + \theta_E^*}{2}\right) \right) - \frac{1}{2} \left(\mathcal{L}_e(\theta_e^*) + \mathcal{L}_E(\theta_E^*) \right) \quad (162)$$

$$\leq \frac{1}{2} \times \left(\frac{1}{2} L \left\| \frac{\theta_E^* - \theta_e^*}{2} \right\|_2^2 \times 2 \right) \quad (163)$$

$$= \frac{1}{8} L \|\theta_E^* - \theta_e^*\|_2^2 \quad (164)$$

Therefore,

$$\mathcal{L}_E(\theta_e^*) - \mathcal{L}_E(\theta_E^*) \geq \frac{\mu \|\theta_E^* - \theta_e^*\|_2^2}{2} \quad (165)$$

$$\geq \frac{\mu}{2} \frac{8D_H(\mathcal{P}_e, \mathcal{P}_E)}{L} = R. \quad (166)$$

□

D. Broader Impact

This paper presents a novel definition of fairness via agent-level awareness for federated learning, which considers the heterogeneity of local data distributions among agents. We develop FAA as a fairness metric for Federated learning and design FOCUS algorithm to improve the corresponding fairness. We believe that FAA can benefit the ML community as a standard measurement of fairness for FL based on our theoretical analyses and empirical results.

A possible negative societal impact may come from the misunderstanding of our work. For example, low FAA does not necessarily mean low loss or high accuracy. Additional utility evaluation metrics are required to evaluate the overall performance of different federated learning algorithms. We have tried our best to define our goal and metrics clearly in Section 3; and state all assumptions for our theorems accurately in Section 4 to avoid potential misuse of our framework.